

TECH. MEMO
AERO 2150

UNLIMITED

LR110498

TECH. MEMO
AERO 2150

DTIC FILE COPY

(2)



ROYAL AEROSPACE ESTABLISHMENT

WEAPON AERODYNAMICS OVERVIEW

by

D. N. Foster

January 1989

19981021 001

Supersedes

AD-A211579

DECLASSIFICATION STATEMENT A
Approved for public release
Distribution Unlimited

Procurement Executive, Ministry of Defence
Farnborough, Hants

UNLIMITED

89 8 22 009

UNLIMITED

ROYAL AEROSPACE ESTABLISHMENT

Technical Memorandum Aero 2150

Received for printing 16 January 1989

WEAPON AERODYNAMICS OVERVIEW

by

D. N. Foster

SUMMARY

The objective of this Memorandum is to highlight the problems currently facing the weapon aerodynamicist; the origins of these problems, and the methods available to predict and to solve the problems.

* Paper presented to the RAeS One-Day Conference on Weapon Aerodynamics, 1 December 1988.

Copyright
©
Controller HMSO London
1989

UNLIMITED

NAME	DRY	1
DATE	12	11
UNCLASSIFIED	11	11
CLASSIFIED		
BY		
DATE		
2. 10/12/1988		
10		
A-1		

Reproduced From
Best Available Copy

LIST OF CONTENTS

	<u>Page</u>
1 INTRODUCTION	3
2 EXPERIMENTAL PROGRAMME FOR FORCES AND MOMENTS	4
3 INVESTIGATIONS OF THE FLOWFIELD	5
4 PREDICTION OF FORCES AND MOMENTS	6
5 KINETIC HEATING	9
6 VERY HIGH ANGLES OF INCIDENCE	11
7 INTAKES	12
8 NON-CIRCULAR BODIES	15
9 STEALTH	16
10 CONCLUSIONS	17
List of symbols	18
References	19
Illustrations	Figures 1-37
Report documentation page	inside back cover

1 INTRODUCTION

As the technology standard of weapons has advanced, as for any airborne system, so the problems facing the specialist have changed. The reasons for the changes in the problems that confront the weapon aerodynamicist are numerous, and vary with the class of the weapon.

For the most prolific class of weapons - the rocket-propelled missile - there are, perhaps, three main reasons for the changes. The first reason is the widening range of configurations currently being considered. The missiles of this class which entered service with the British Armed Forces in the late 1950s and early 1960s - Fig 1 - Thunderbird; Sea Slug, and Firestreak - all had similar configurations: a body of circular cross-section with an ogival or conical nose; cruciform wings of low aspect ratio, with the 50% chord line unswept, and with aft-mounted control surfaces well separated from the wings. There were minor variations of planform, and in the ratio of wing or control surface span to body diameter.

More recent weapons have shown more significant variations of configuration, Fig 2. Thus Rapier has a wing with a highly swept leading edge, while Sea Wolf has a similar delta planform wing, but with the wing to control surface gap reduced. ASRAAM has dispensed with wings altogether, whilst Javelin has small canard control surfaces and larger rear wings.

As well as being faced with a wider range of configurations, the weapon aerodynamicist now has to deal with a wider range of Mach numbers. The first generation weapons had maximum Mach numbers of the order of 2. More recent projects have maximum Mach numbers in excess of 4, partly to reduce flight time, and, for those weapons which rely on a kinetic energy kill, to increase lethality. This brings kinetic heating into the span of problems facing the weapon aerodynamicist.

The third factor is the increase of manoeuvrability demanded of the missile. Recent advances in fighter design have resulted in the target aircraft having much enhanced manoeuvrability - up to the physiological limit of the pilot. However, much more significant is the fact that missiles have now to intercept other missiles, which, being pilotless, do not recognise any physiological limit. These demands for increased missile manoeuvrability translate into increased normal forces and the need for well-ordered development of the flow around the missile as angle of incidence increases.

2 EXPERIMENTAL PROGRAMME FOR FORCES AND MOMENTS

In response to these new challenges both RAE and BAe Dynamics Division set up research programmes in the early 1980s.

The RAE programme¹ centred around the recommissioned High Supersonic Speed Tunnel (HSST) at RAE Bedford. This is a continuous flow wind tunnel with a working section 3ft x 4ft (0.91m x 1.22m), capable of testing over the Mach number range of 2.5 to 5. To avoid condensation shock waves at Mach 5 the stagnation temperature needs to be raised to around 140°C. The strain gauge balances used would not accept this high temperature, and so the maximum Mach number has been limited to 4.5. Fig 3 shows the wide range of isolated bodies and body-wing configurations to be tested in this programme. Combinations of three nose shapes; six body lengths and 12 wing shapes are possible. Control surfaces with a range of planforms can also be installed at typical forward or aft locations on the cylindrical section of the body. Overall loads on the complete model; loads on two opposing wing panels, and loads on two opposing control panels can be measured.

BAe also undertook a programme² in their Guided Weapon Wind Tunnel (GWWT) at Warton under RAE sponsorship. This is a blowdown facility with a working section 18in x 18in (0.457m x 0.457m), capable of test Mach numbers from 1.7 to 6.0. The BAe programme was more sharply focussed, Fig 4, and investigated the effects of forebody and afterbody length on the aerodynamic characteristics of a body and a 70° delta wing.

Some results from these programmes are shown in the next four Figures. Fig 5 shows that the effect on normal force of increasing the length of the forebody for the isolated body (B1A to B5A) is, typically, increased by some 3% when wing W13 is added to the bodies (B1AW13 to B5AW13). In contrast the addition of wing W14 to bodies B5A and B11A, Fig 6, reduces the effect of the increase of forebody length by typically 8%.

Analysis of the wing panel loads, Fig 7, shows that the wing loads are independent of forebody length, for the configurations shown. The only effect of forebody length is an increase of overall normal force due to the additional body length.

Fig 8 shows that the effect of increasing afterbody length on normal force for the isolated body (B1A to B5A) is, typically, increased by some 25% when wing W14 is added to the bodies (B1AW14 to B5AW14A3). The wing loads are the same as

the nose and forebodies are identical. Thus the increase is due to the carry-over of normal force from the wing onto the body being greater when an afterbody is present.

3 INVESTIGATIONS OF THE FLOWFIELD

Overall and panel load tests as described above can indicate the effect of geometric changes on the aerodynamic characteristics, but cannot give an explanation of why the effects occur. To obtain this information more fundamental measurements of the flowfield are required. At RAE two programmes are being pursued; one is an investigation of the flowfield above the missile, whilst in the other the pressure distribution over the surface of a typical missile is being measured.

Measurements of the flowfield above the weapon have been made using five-hole yawmeters, Fig 9. From the pressures measured by the yawmeters, and their calibrations, the total pressure; flow angles (flow plane angle and total flow angle), and the Mach number at the measurement point can be derived. Subsequent analysis yields values of the velocity components and vorticity at the measurement point and the overall circulation. To date tests have been conducted in the RAE 8ft x 8ft Tunnel at Mach numbers up to 1.8. Development work is underway³ to allow tests in the RAE 3ft x 4ft Tunnel, to enable these measurements to complement the surface pressure measurements.

Fig 10 shows a typical cross-flow Mach number distribution measured at one longitudinal station at an angle of incidence of 14° and a free-stream Mach number of 1.8. A vortex can be clearly seen, located at about 160° from the windward generator. By tracing the vortex feeding sheet back to the surface it is clear that the flow has separated from the surface of the body at about 110° from the windward generator. Along the leeward generator and close to the surface of the body the vortex has induced a flow with a small component of velocity towards the surface; between the leeward generator and the separation point the flow direction reflects the rotation of the vortex.

At the same longitudinal station and Mach number, but at a lower angle of incidence of 8° , Fig 11, the vortex is still present, although less intense and closer to the surface of the body. At an angle of incidence of 20° , Fig 12, the vortex is more intense and is further from the surface of the body, but it has now lost its circular shape and become elliptical.

Fig 13 shows how the pressure measurement programme is broken down. Tests have already been conducted to measure the static pressure around the circumference

of an isolated body at a range of stations along the body. Tests on the pressure-plotted nose are scheduled to take place in the RAE 3ft x 4ft Tunnel, at Mach numbers between 2.5 and 4.5, in December 1988, with further tests in the RAE 8ft x 8ft Tunnel, at Mach numbers below 2.5, in April 1989. Testing of the pressure-plotted body and wing will commence in the 3ft x 4ft Tunnel in September 1989.

Fig 14 shows a typical pressure distribution measured at one longitudinal station at an angle of incidence of 14° , and a Mach number of 2.5⁴. The density of pressure-plotting points allows the main features of the flow to be identified. From the windward generator the flow expands steadily until an angle of about 90° is achieved, when a cross-flow shock wave occurs. The vortex flow-field measurements have shown that the flow then separates from the surface. From the leeward generator the flow velocity induced by the vortex increases to a position below the vortex ($\phi = 160^\circ$), and then reduces as the separation position is approached.

Fig 15 shows contours of constant values of pressure coefficient derived from the full set of pressure measurements along the body, again at an angle of incidence of 14° and a Mach number of 2.5. Noteworthy is the fact that the contour pattern varies little from the 9.5 calibre station to the furthest measuring station. The cross-flow shock wave appears to be slightly more to leeward near the junction of the body and the nose, presumably due to the influence of the nose. Immediately beyond the cross-flow shock wave there is a region of constant pressure, and thus of velocity, which is present all along the body. However the effect of the vortex on the surface pressures is a maximum at the 5.5 calibre station, and decreases downstream. This is considered to be due to the convection of the vortex away from the surface of the body.

Fig 16 gives an overall impression of the flow around a missile at moderate to high angles of incidence. Separations from the nose give rise to a pair of vortices above the body, which pass close to the vertical wings and control surfaces. At high angles of incidence the flow is likely to be separated from the leading edges of the horizontal wings with a vortex lying over the leading edge and being shed from the tip of the wing. Altogether the flowfield at high angles of incidence will be dominated by vortices.

4 PREDICTION OF FORCES AND MOMENTS

There are basically two classes of prediction methods for the forces and moments experienced by weapons - semi-empirical and Computational Fluid Dynamics.

Semi-empirical methods use the building-block approach. The forces and moments on each component in isolation are first calculated, and the characteristics of the complete configuration is then obtained by summing the component values and calculating the mutual interference between components. The component loads and the mutual interference terms are obtained primarily from slender body theory and linear theory, suitably factored to reflect experimentally-derived values. Semi-empirical methods can only, therefore, be used with confidence for weapons having geometries similar to those from which the factors were derived. Equally, it is possible to 'tune' semi-empirical methods to particular configurations which other methods could not tackle.

In Computational Fluid Dynamics (CFD) methods the fundamental equations for the flow around the weapon are solved, with some approximations. Once the solution is established the flow properties all over the surface of the weapon can be calculated, and from predictions of surface pressures component loads and overall forces and moments may be derived. In principle CFD methods can be applied to any configuration without reference to previous experimental measurements on configurations having similar geometries. In practice, validation is required of the approximations needed to enable a solution to be achieved, and this is undertaken against high quality experimental data. Once this validation has been completed the CFD methods can be applied with confidence to a wide range of configurations.

As an indication of the accuracy of typical examples of the two classes, Fig 17 compares the prediction of a semi-empirical method developed by BAe Dynamics Division - Abacus⁵ - and a CFD method developed by the US Naval Surface Warfare Centre - SWINT⁶ - with experimental measurements for a body-wing configuration at a Mach number of 3.5. The two predictions agree well with the experimental values of normal force at angles of incidence up to 12°, but at the higher angles of incidence - the most critical region from the viewpoint of flight performance - SWINT is more accurate. SWINT also gives better predictions of the centre of pressure, and so would give more accurate predictions of longitudinal stability.

One of the improvements which has been made to SWINT in the UK is the addition of a facility to model the interaction of body vortices with downstream lifting surfaces, and to calculate the loads on control surfaces. Fig 18 shows the loads measured on a deflected control surface as the configuration is rolled through 360°, and includes the predictions from Abacus and SWINT. The semi-empirical method performs fairly well, but it fails to reproduce the interaction

of the body vortices with the fins when they are in the leeward position - a feature which is well picked up by SWINT.

Up to quite high angles of incidence axial force varies only slowly with angle of incidence, and for performance calculations can be characterised by the value at zero angle of incidence - the zero incidence drag. There are three components of zero incidence drag - pressure drag, skin friction drag and base drag. CFD methods which solve the Euler equations can only predict the pressure drag, and so semi-empirical methods⁷ are employed to predict the sum of the pressure drag and skin friction drag. As above, the semi-empirical methods are built around the individual component contributions as measured experimentally, together with interference factors.

Base drag can account for about 30% of the overall drag for a typical missile configuration. Two semi-empirical methods for the prediction of base drag at supersonic speeds^{8,9} have been developed in the US. Fig 19 shows a correlation of the predictions of these codes with measured values of base pressure coefficient for a range of jet pressure ratios; jet Mach numbers and free stream Mach numbers¹⁰. For some configurations the predictions were in reasonable agreement with the experimental results, but equally there were configurations for which the predictions were grossly in error, and for some configurations no solution was possible. It is clear, therefore, that the methods have to be used with caution.

In addition to the prediction of the forces and moments for the weapon in a fixed attitude - the so-called static derivatives - estimations of the flight trajectory, including manoeuvres, require predictions to be made for conditions where the attitude is changing with time - the dynamic derivatives. Fortunately, perhaps, the equations of motion of a weapon tend to be dominated by the static derivatives, and so a lower accuracy for the prediction of the dynamic derivatives is acceptable.

Dynamic effects are related to the 'reduced frequency', defined as

$$\frac{\text{angular rate} \times \text{characteristic length}}{\text{flight velocity}}$$

For weapons at low angles of incidence the reduced frequency is normally small, and the motion can be assumed to be quasi-steady. Under this assumption the time dependent motion is assumed to be a small amplitude sinusoidal oscillation; thus a pitching motion would add a small angle of incidence, varying along the length of the body, to the constant angle of incidence due to the flight velocity.

Schneider¹¹ has given a thorough review of the methods for the prediction of dynamic derivatives.

In general separated flows are more frequency dependent than attached flows. At high angles of incidence, when the flowfield is dominated by separated flow, dynamic effects are likely to be more significant, and quasi-steady assumptions will not apply.

The load distribution over the length of a missile changes with acceleration or deceleration. A missile which is subject to a high acceleration at low speeds may therefore experience a significant rearward movement of the centre of pressure during this phase of the flight.

5 KINETIC HEATING

Kinetic heating effects are most significant at the nose of a missile and along the leading edges of wings and control surfaces. Weapons designed for flight at high Mach numbers at high altitude are likely to experience kinetic heating over a period of time long enough for the structural temperature to rise to a level at which transparencies in the nose may become opaque or crack, and leading edges may distort under the aerodynamic loads. Although weapons designed for flight at low altitude may have short times of flight, the accelerations envisaged to the high terminal Mach number - figures of 50 'g' and 100 'g' have been mentioned - will bring with them problems of thermal shock even if in the short time of flight the structure does not reach an equilibrium temperature.

As well as the problem of predicting kinetic heating rates there are also problems in establishing experimental values to validate prediction methods. The facilities at RAE in which measurements may be made were constructed some years ago for research at hypersonic speeds. Whatever the definition of hypersonic speeds these facilities would have met it, as all operated at Mach numbers greater than 10. The Shock Tube, Fig 20, as originally operated in the 1960s, could operate at Mach numbers of 10 and 13. It used nitrogen as the test gas with hydrogen as the driver gas. The running time was of the order of 3 to 10 ms, but this was sufficiently long to allow heat transfer measurements to be taken.

In order to be able to operate at Mach numbers more appropriate to High-Speed Weapons, and at the same time to extend the running time so that measurements of forces and pressures could be made as well as heat transfer, the facility is being modified in two stages.

The first version is the LICH tube - LICH standing for Ludwig Isentropic Compression Heating, Fig 21. Nitrogen is used as both the driver gas and the test gas. When the required pressure is achieved in the driver section the tail valve is opened and the non-metallic piston moves into the driven section. When it has increased the pressure in the test gas sufficiently the fast-acting valve opens, and the test gas discharges through the nozzle and test section. A running time of 100 ms is achieved in this mode. Having the test gas at room temperature is sufficient to avoid liquefaction of the gas in the test section at a Mach number of 7, and operating just above the liquefaction temperature gives the highest possible Reynolds number in the test section. For tests at a Mach number of 9 it is necessary to heat the test gas to 140°C by an electrical heater wrapped around the driven gas reservoir in order to ensure that liquefaction problems will not be encountered.

In principle the LICH mode could also be used for operations at a Mach number of 5, more relevant to high speed weapons of the immediate future. For this Mach number a reservoir temperature of 250°C is required to prevent liquefaction in the test section. However, the piston travels at about 50 m/s when operating at a Mach number of 7; the higher mass-flows inherent in operating at a Mach number of 5 (increased by a factor of at least 4) will result in a significantly higher piston speed, with the result that stopping the piston becomes very difficult, and there is a high probability that the piston will be destroyed on impact with the downstream end of the tube. A different mode is therefore required for Mach 5. This is the Ludwig Tube, Fig 22. There is now only one reservoir, and the test gas is again heated by the wrap-around electrical heater. Conditions in the test section are constant for the order of 100 ms whilst the expansion wave generated by opening the fast-acting valve travels to the upstream end of the reservoir and returns to the valve. One attraction of this mode is that for very high reservoir pressures - of the order of 6000 psi - near full-scale Reynolds numbers will be achieved in the test section. This is particularly important for heat transfer measurements which are difficult to scale with Reynolds number.

Heat transfer tests are currently being undertaken over a range of Mach numbers using a technique developed by the late Professor Schultz and his co-workers at the Department of Engineering Science at Oxford University¹². A typical model is shown at Fig 23. A machineable glass ceramic - MACOR - is used as the substrate, and short lengths of platinum are used as the heat transfer gauges. The gauges are connected via low resistance conducting strips of gold to wiring internal to the model. The advantage of this technique is that

the heat transfer gauges can be closely packed - in the case of this model 36 gauges in a length of 6 in. Testing of this model will produce high quality data against which prediction methods can be validated. Fig 24 shows that the prediction method KHOMP2D developed by Hellon and Poll¹³ gives very good agreement with measured values at zero angle of incidence.

6 VERY HIGH ANGLES OF INCIDENCE

Turning from high Mach numbers to very low speed, one recent development has been the introduction of Vertical Launch. This concept allows an anti-missile missile, for example, to intercept an attack coming from any direction regardless of the orientation of the launch platform. An example of this concept is Vertical Launch Sea Wolf. When launched from a fixed platform in still air the missile will fly at a low angle of incidence, but when used operationally it would be launched from a ship travelling at perhaps 30 kn, so that when the missile is in the early part of its launch trajectory with a low forward speed very high angles of incidence will be experienced. Similar high angles of incidence may be experienced in the turn-over manoeuvre to intercept sea-skimming missiles.

The problems that arise at high angles of incidence have been investigated on a number of occasions, including tests of this model, Fig 25, in the RAE 5m pressurised Low-Speed Tunnel¹⁴. Tests such as these, Fig 26, indicate that whilst the in-plane forces increase steadily with angle of incidence at a given orientation there is no out-of-plane force up to, in this instance, 20°, subsequently the out-of-plane forces increase rapidly with angle of incidence. Fig 27 shows that, at a very high angle of incidence, as the model is rolled the out-of-plane forces switch rapidly and erratically from one 'fully-asymmetric' value to another.

Recent theoretical analysis¹⁵ has shown the existence of a stable, asymmetric solution for the vortex sheets shed from symmetric positions on the conical nose. Fig 28 shows a typical theoretical solution, and also suggests that for elliptic cross-section cones the asymmetry reduces and finally disappears when the eccentricity of the ellipse reaches a certain value. These theoretical solutions can explain the existence of the 'fully-asymmetric' values of out-of-plane forces; the variation with roll angle would appear to result from very minor imperfections near to the nose of the cone. Various palliatives for this effect have been suggested - achieving an out-of-plane force that is always at the 'fully-asymmetric' value; reducing the out-of-plane force to zero, or allowing the out-of-plane force to be controlled to any required value.

By attaching an excrescence to the nose of a sharp cone it is possible to swamp any minor manufacturing errors in the nose, and to generate reliable and repeatable out-of-plane forces at the 'fully-asymmetric' level at all roll angles¹⁶. The excrescence should be attached very close to the tip of the nose and at an angle between 90° and 150° from the windward generator. If the nose tip is blunted the 'fully-asymmetric' value of the out-of-plane force is reduced slightly, but the forces still show a random dependence on roll angle. The attachment of an excrescence can again remove the dependence on roll angle, but very precise positioning of the excrescence is required.

For concepts which do not require a sensor in the nose of the missile an alternative solution has been proposed. Tests have been conducted on a model which had a short section of the nose free to rotate, this nose section having two sharp-edged strakes set at a dihedral angle¹⁷. It was found that the nose portion weathercocked to an attitude symmetric about the cross-flow plane, whatever the roll orientation of the body, with the result that the out-of-plane forces varied little with roll angle. In comparison with the body without strakes, the onset of out-of-plane forces was delayed to a higher angle of incidence and the magnitude of the out-of-plane forces was reduced.

The use of air jets blowing through an orifice close to the tip of the nose has also been investigated¹⁸. When blowing from an orifice located at an angle of 150° from the windward generator, very small quantities of blowing air have been found to have large effects on the aerodynamic characteristics. In addition to eliminating the out-of-plane forces, the possibility exists of using the jet as a control device by varying the blowing rate to achieve the out-of-plane forces required for manoeuvres.

7 INTAKES

To this point the discussion has centred on problems associated with rocket-propelled weapons. However, air-breathing propulsion also has a part to play in weapon design, particularly when extended range is required. Air-breathing propulsion featured in the early Surface-to-Air missile Bloodhound, and the later Sea Dart, Fig 29. In Bloodhound the Thor ramjets were mounted in nacelles, whilst Sea Dart was built around the Odin ramjet. Both these weapons required separate, jettisonable booster rockets to accelerate the weapon to the ramjet self-sustaining speed.

Future designs may feature a single, central engine (as in Sea Dart) but with intakes mounted on the side of the body to leave the nose free for guidance

equipment. It is possible also that a combined rocket-ramjet propulsion system will be used. Cartesian-controlled missiles (ie those which can generate substantial acceleration in any lateral direction) experience incidence at any roll angle. Thus it is generally necessary to use multiple side intakes to minimise the sensitivity of the propulsion system to roll angle. For twist-and-steer missiles, side mounted twin intakes are adequate, as the possible range of flow directions is more limited.

RAE has carried out research on both the internal performance of a range of side intakes mounted on a representative missile body, and on the effect of the intakes on the aerodynamic characteristics of the missile¹⁹. Fig 30 shows the number; size; shape, and location of the intakes which could be mounted on the 'aerodynamic characteristics' model; wings of cropped delta planform and control surfaces could also be added.

Fig 31 shows the effects of adding intakes to the isolated body. The rectangular intakes (having an entry area 50% of the body reference area) contribute some 60% of the total normal force. Rectangular intakes are significantly more effective in producing normal force than half-axisymmetric intakes with the same entry area, although the rectangular intakes do have 25% more planform area. It is interesting that the smaller half-axisymmetric intakes, with only half the entry area, produce normal forces similar in magnitude to the larger intakes.

One problem encountered with side intakes is that at certain combinations of angle of incidence and roll angle the vortices shed from the forebody can enter the intakes, to the detriment of intake performance. Tests on the 'intake performance' model have shown that small strakes, mounted on the forebody and aligned with the intake axis, modify the trajectories of the vortices, and improve overall intake performance. The 'aerodynamic characteristics' model has shown that the strakes do not, in general, give strong adverse aerodynamic effects. They do, however, generate significant side forces at non-symmetrical roll angles, which appear to arise both from flow asymmetry around the body and from the resolved strake forces.

A semi-empirical prediction method for side intake configurations has been developed by BAe Dynamics Division based on Abacus²⁰ in a cooperative programme of research with RAE. In line with the original method, the intake section loads are comprised of a linear part (a modified potential flow term), and a nonlinear part (a viscous term arising from flow separations) which employs cross-flow drag terms developed from the 'aerodynamic characteristics' tests. Fig 32 shows that the resultant prediction method gives good agreement with experimental results

not used in the derivation of the method. Overall the method is considered to be capable of predicting normal force to within 10% of measured values; predictions of the centre of pressure position are also reasonable, with the possible exception of the twin ventral intake configuration, which produces significant lift at zero angle of incidence due to intake asymmetry.

As the IN in SWINT stands for Inlet this CFD method has a basic capability of dealing with intakes. Fig 33 shows a comparison of the predictions of SWINT with experimental results for a configuration with twin half-axisymmetric ventral intakes²¹. Some small modifications of the geometry were required in order to obtain results from SWINT, and a solution was not possible at an angle of incidence greater than 9° ; it was thought that this was due to the appearance of a subsonic patch in the flow - the free-stream Mach number of 2.3 is relatively low for SWINT. Over the range of angles of incidence for which SWINT solutions were obtained the predictions of normal force are in reasonable agreement with the experimental results. The predicted trend of the position of the centre of pressure with angle of incidence differs from the experimental trend; the experimental data have not been corrected for the contribution to pitching moment from the intake internal flow momentum, and are therefore strictly not comparable with the SWINT predictions, which exclude intake momentum effects. However, it is believed that these effects are likely to be small (around 10% of centre of pressure position), and so the discrepancies are due primarily to the inability of the code to model viscous effects.

The configuration to which SWINT has been applied was chosen carefully; use of SWINT for a configuration with rectangular intakes is likely to require more extensive modifications to the actual geometry, and to result in less accurate predictions, due to enhanced viscous effects, with the flow separating from the corners of the intakes. Configurations with intakes are therefore an example of where a 'tuned' semi-empirical method currently has more widespread applicability than a CFD method.

For one class of weapon - the Stand-Off Missile - designed for long range at very low altitude, turbofan propulsion is really the only choice. Fig 34 shows a typical Stand-Off Missile - Sea Eagle. Here the aerodynamic problems lie primarily with the intake aerodynamicist - achieving adequate flow quality at the engine face with an intake which is short and sharply curved. Apart from the effect of the intake, it should be possible to predict the overall aerodynamic characteristics using the wealth of prediction methods built up for subsonic air

vehicles. The effect of the intake is likely to be small and limited to changes in pitching and yawing moments.

8 NON-CIRCULAR BODIES

One design feature which has had a profound effect on the problems facing the aerodynamicist is the change of warhead of the Stand-Off Missile from unitary - as in the Sea Eagle - to submunitions or bomblets. Packaging of submunitions has led to a change of body cross-section shape from the traditional circle to a square. A typical layout, Fig 35, is shown by this model of an unpowered Stand-Off Missile tested in the RAE 8ft x 6ft Wind Tunnel as part of an investigation into the possibility of the weapon being released from an underwing pylon and subsequently following an upward trajectory through the wake of the wing of the carrier aircraft²².

The layout features a square cross-section body with the wing and the horizontal control surfaces mounted at the top of the body to allow unrestricted installation of the submunitions. The sharp corners of the body result in flow separations and the appearance of vortex sheets from comparatively low angles of incidence, Fig 36, affecting both the forces generated by the body and the flow-fields around the wing and the horizontal control surfaces. Overall, the in-plane forces and moments are likely to be nonlinear. When the body is rolled the flow patterns change significantly, but become symmetrical again when the roll angle reaches 45° . Thus the out-of-plane forces and moments are likely to be strongly dependent on roll angle.

The prediction of the forces and moments on the square-bodied configuration requires some modifications to existing prediction methods. Isaacs has extended the method he has developed for carriage load prediction^{23,24} so that, initially, the potential flow loading is calculated on an equivalent axisymmetric body with a mid-mounted wing and horizontal control surfaces. The diameter of the body is equal to the width of the square body; the chord length and gross semi-span of the wing and control surfaces are modelled correctly. The potential flow loading on the body is calculated by exact linear theory, and wing and control surface loadings include all wing-body effects and nonlinear loadings due to leading-edge and tip-edge effects. The interference loading on the horizontal control surfaces due to the wing trailing vortices is also calculated. The calculated coefficients are then broken down into their constituent parts - body potential loading; body nonlinear loading; wing loading and control surface loading. The body nonlinear loading is factored in the ratio of the cross-flow drag coefficients for square and circular bodies. All other components are factored using

the ratio of the loadings calculated by slender-body theory²⁵ for the square body (either alone or with a high wing or high control surfaces) to the circular body (again alone or with a mid-wing or mid-control surfaces).

Fig 37 shows a comparison of the predictions derived in this way with experimental results measured at a Mach number of 0.6. There is good agreement between the predicted and measured normal force up to at least an angle of incidence of 10° . The prediction of the position of the centre of pressure is less good - examination of the loadings measured in build-up tests (body + wing; body + control surfaces) suggests that at the higher angles of incidence the predicted control surfaces loading is not realised in practice. This loss of loading is presumably due to the presence of the body vortices, and would have only a small effect on normal force but a significant effect on pitching moment, and thus on centre of pressure.

9 STEALTH

In the future configurations may be affected by stealth considerations, and hence the aerodynamicist will face new challenges. Stealth considerations are unlikely to affect all classes of weapons - those which are physically small and have short times of flight have low probabilities of detection, and are unlikely to be affected significantly. The primary class of weapons which will be affected will be the Subsonic Stand-Off Missile with comparatively long flight times.

Some measures to minimise signatures, such as the elimination of engine exhaust smoke to reduce visual signature, or reducing the extent of emissions from sensors forming, for example, part of a terrain matching system, have no effect on the aerodynamic configuration. For the subsonic missile the infra-red signature will be predominately in the rear hemisphere. In order to minimise the IR sensor's view of the hot metal in the engine bay, a shield can be installed around the jet pipe. If it is possible to be certain of the direction of the threat - eg from an Infra-Red Search & Track (IRST) sensor carried on a fighter on Combat Air Patrol (CAP) at medium altitude when the missile is penetrating at low altitude - then a shield extending rearwards over the jet pipe is appropriate. If the threat could be from any direction then a rectangular nozzle of moderate or high aspect ratio is required. If further reduction of the IR signature is required then one could envisage auxiliary intakes admitting additional cool air, and intense mixing within the airframe, so that as uniformly mixed an efflux as possible is produced - not easy in a small missile.

As far as reduction of radar signature is concerned, there are some well-known guidelines for reducing signatures. Right angle junctions should be avoided, leading to blended wing-bodies and twin, inclined fins. For flying surfaces and intakes straight leading edges should be avoided, as they give significant returns when the incident radar beam is normal to the leading edge. Hence leading edges should be curved. The intake duct is a significant source of returns - even if there is no direct view along the duct to the engine face the duct walls will act as a waveguide and direct the incident signals towards the compressor, which will then reflect them back up the duct to the radar receiver. Treatment of the duct walls with Radar Absorbent Material (RAM) could alleviate this effect, but the missile design may be compromised by the additional mass of the RAM. An alternative approach might be to rely on the hypothesis that radar waves will not enter a duct whose height is less than the wavelength of the incident beam. This implies a very high aspect ratio inlet.

The integration of these concepts in a practical missile capable of achieving the required mission profile will not be easy - problems with stability and control and with intake flow will be particularly difficult to solve. It must also be recognised that whilst the missile in free flight may have a low signature, it could well give a significant increase to the signature of the parent aircraft during the carried part of the mission.

10 CONCLUSIONS

- (1) The extensive database on loads and moments for a wide variety of conventional missile configurations will enable the applicability of semi-empirical methods to be extended, and will contribute to the validation of CFD methods.
- (2) The measurement of flowfield and surface pressure characteristics will further the understanding of the flow around a missile, and will provide more severe test cases for CFD methods.
- (3) The increase of maximum Mach number will put more emphasis on the measurement and prediction of kinetic heating effects.
- (4) Solutions will need to be found to eliminate the random variation of out-of-plane forces generated at very high angles of incidence.
- (5) The effect of intakes on overall aerodynamic characteristics is large, but may be beneficial.
- (6) Significant aerodynamic problems, requiring extensive aerodynamic research, may be encountered for unconventional shapes.

LIST OF SYMBOLS

C_n	overall normal force coefficient
C_{np}	panel normal force coefficient
C_p	pressure coefficient
C_{pb}	base pressure coefficient
C_Y	side force coefficient
D	maximum body diameter
M	freestream Mach number
\dot{q}	local heat transfer rate
\dot{q}_0	heat transfer rate at stagnation point
X	axial location relative to body nose
X_{cp}	overall longitudinal centre of pressure location/maximum body diameter
ζ	rudder angle
λ	body roll angle
σ	angle of incidence to freestream
ϕ	angular position on body surface

REFERENCES

<u>No.</u>	<u>Author</u>	<u>Title, etc</u>
1	J. Hodges L.C. Ward	The RAE Experimental Data-Base for Missiles at High Mach Number and its use in assessing CFD Methods. <i>Aerodynamics of Hypersonic Lifting Vehicles</i> , AGARD CP-428, pp 32-1 to 32-14, April 1987
2	P.G.C. Herring	A Programme of Wind Tunnel Tests on Wing-Body Configurations at Speeds up to Mach 5.5. BAe DG Bristol JS 10534, February 1986
3	T.J. Birch	Private Communication. RAE (1988)
4	L.C. Ward	The experimental pressure distribution at one location around a body at Mach numbers from 2.5 to 4.5. RAE Technical Memorandum 2120 (1988)
5	P.G.C. Herring	'Abacus' - A Computer Program which evaluates the Longitudinal Aerodynamic Characteristics of Weapon Configurations. BAe DG Bristol ST 14275, September 1975
6	A.B. Wardlaw Jr F.P. Baltakis J.M. Solomon L.B. Hackerman	Inviscid Computation Method for Tactical Missile Configurations. NSWC TR 81-457, December 1981
7	P.C. Dexter P.G.C. Herring	A Computer Program which Evaluates the Zero Incidence Drag of Weapon Shapes at Subsonic, Transonic and Supersonic Speeds. BAe DG Bristol ST 19372, February 1978
8	T.H. Moulden	Guide to the Operation of the MICOM/UTSI Computer Program for the Plume Induced Separation at Transonic Speeds: Version 2. US Army Missile Command, Redstone Arsenal, TR-RD-CR-81-2 (1980)

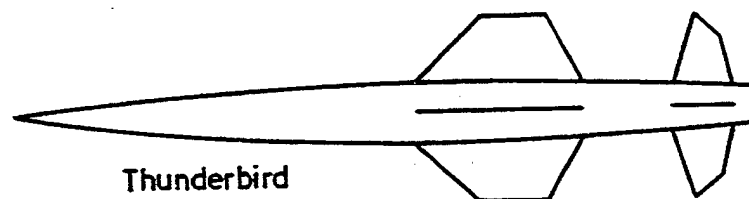
REFERENCES (continued)

<u>No.</u>	<u>Author</u>	<u>Title, etc</u>
9	A.L. Addy	Analysis of the Axisymmetric Base Pressure and Base Temperature Problem with Supersonic Inter-acting Free Stream Nozzle Flows based on the Flow Model of Korst <i>et al.</i> US Army Missile Command, Redstone Arsenal, RD-TR-80-12, July 1969
10	T.W.F. Moore	Further Studies of Computer Codes for Base Flows with Centred Propulsion Jets. BAe SRC Bristol JS 10864, October 1987
11	C.P. Schneider	Presentation of Stability Derivatives in Missile Aerodynamics and Theoretical Methods for their Prediction. <i>Dynamic Stability Parameters</i> , AGARD CP-235, pp 20-1 to 20-31, May 1978
12	M.L.G. Oldfield T.V. Jones D.L. Schultz	'On-line Computer for Transient Turbine Cascade Instrumentation'. <i>IEEE Transactions AES</i> , <u>14</u> , 738 (1978)
13	C.M. Hellon D.I.A. Poll	On the Use of the Boundary Layer Integral Equations for the Prediction of Skin Friction and Heat Transfer. Cranfield CoA Report No.8625, March 1987
14	I.R.M. Moir	Private Communication. RAE (1988)
15	S.P. Fiddes J.H.B. Smith	Asymptotic separation from slender cones at incidence. RAE Technical Memorandum Aero 2118 (1988)
16	A.R.G. Mundell	Private Communication. RAE (1988)
17	I.R.M. Moir D.H. Peckham J.S. Smith	Low speed wind tunnel tests of a device for reducing the out-of-plane forces on a pointed slender body of revolution at high angles of incidence. RAE Technical Memorandum Aero 1992 (1984)

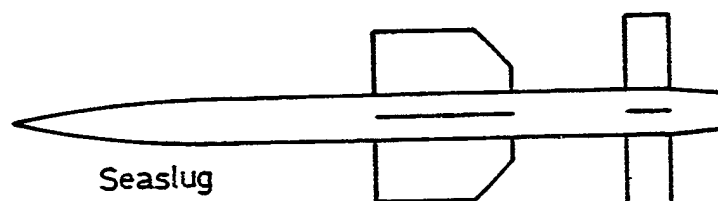
REFERENCES (concluded)

<u>No.</u>	<u>Author</u>	<u>Title, etc</u>
18	A.R.G. Mundell	Low speed wind tunnel tests on the use of air jets to control asymmetric forces and moments occurring on aircraft at high incidences. RAE Technical Memorandum Aero 1984 (1984)
19	G.R. Beaman	A Survey of Research into Aerodynamic Characteristics using RAE Model 2110 - 1982 to mid 1986. BAe NESD Bristol BT 20662, October 1986
20	G.R. Beaman	A Method for the Prediction of Aerodynamic Characteristics of Air Breathing Missiles at Supersonic Speeds - Issue 2. BAe NWD Bristol BT 21168, January 1987
21	B.H. Denchfield	Private Communication. BAe Dynamics Division, 1988
22	R.N.L. Howarth	Investigation of the aerodynamic characteristics of a square-bodied lifting dispenser in the 8ft x 6ft Transonic Wind Tunnel. RAE Technical Memorandum Aero 2100 (1987)
23	D. Isaacs	Store carriage loads at subsonic speeds. Part 1: Prediction of the incidence-dependent loading on isolated axisymmetric bodies. RAE Technical Report 88009 (1988)
24	D. Isaacs	Store carriage loads at subsonic speeds. Part 2: Prediction of store wing and fin loads. RAE Technical Report 88011 (1988)
25	D. Isaacs	A two-dimensional panel method for calculating slender-body theory loading (or loading for minimum vortex drag) on a body of arbitrary cross-section. RAE Technical Report 81003 (1981)

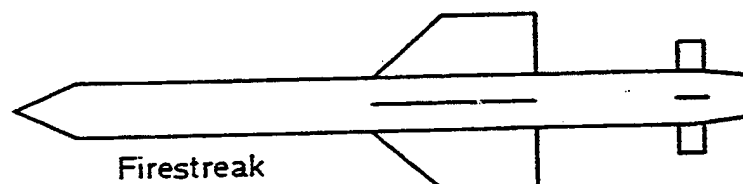
Fig 1



Thunderbird



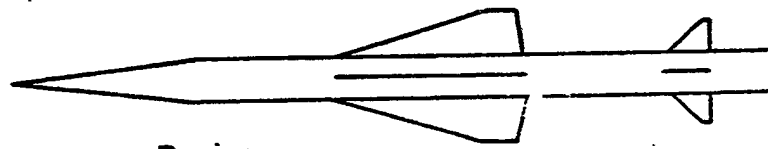
Seaslug



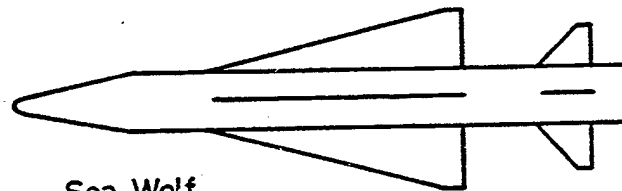
Firestreak

Fig 1 First generation UK rocket-propelled missiles

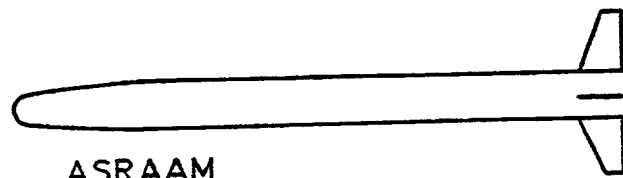
Fig 2



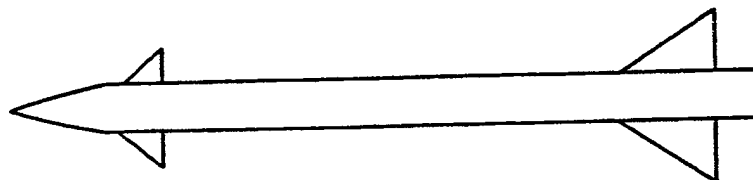
Rapier



Sea Wolf



ASRAAM



Javelin

Fig 2 Current UK rocket-propelled missiles

Fig 3

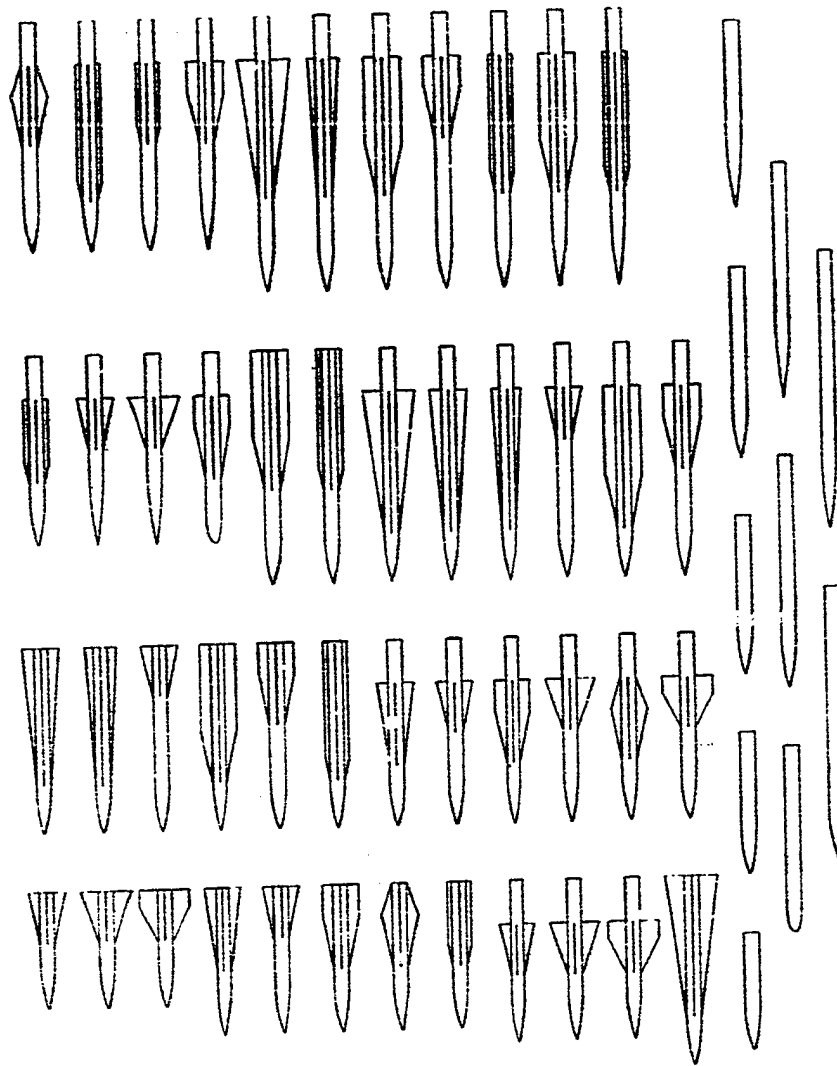
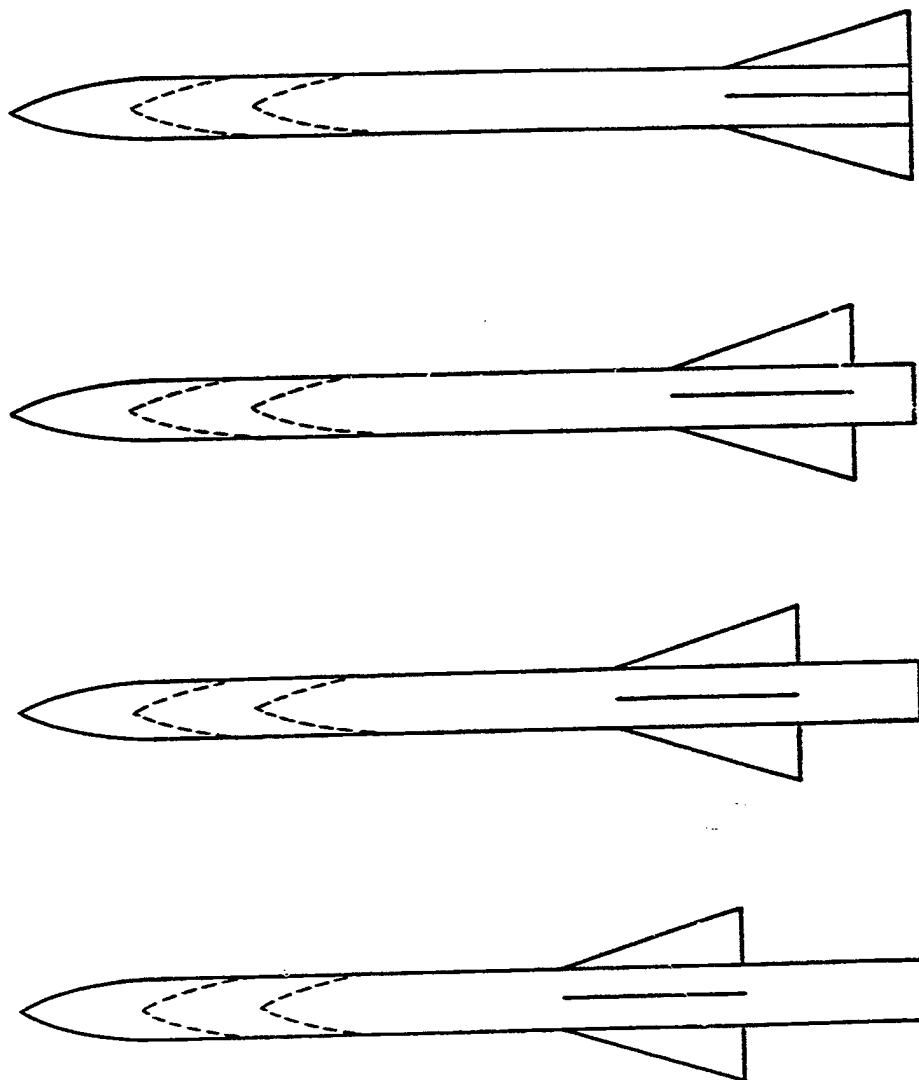


Fig 3 RAE body and body-wing configurations

Fig 4



All bodies have a 2.0 calibre tangent ogive nose

Fig 4 BAe body-wing configurations

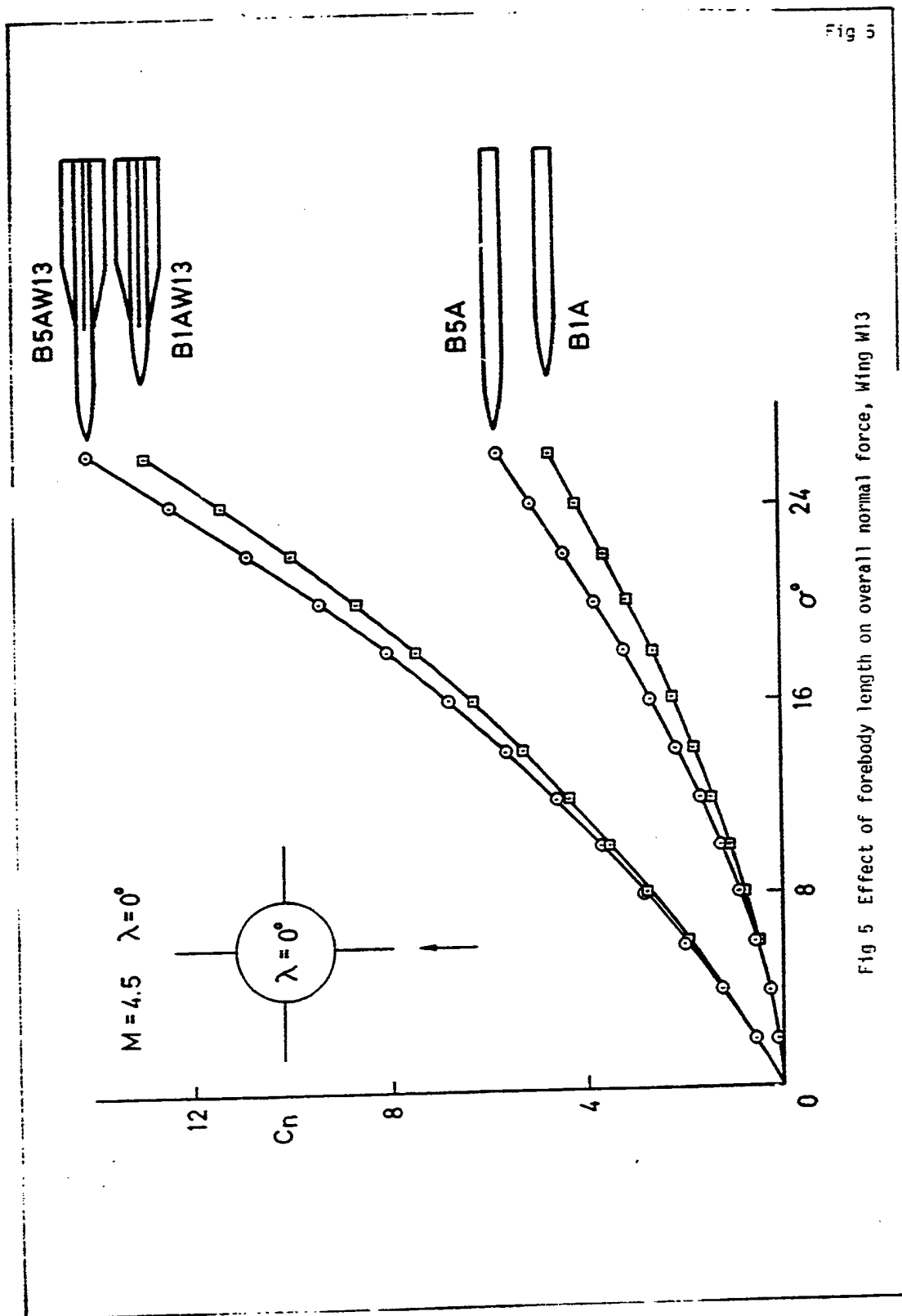


Fig 5

Fig 5 Effect of forebody length on overall normal force, Wing W13

Fig 6

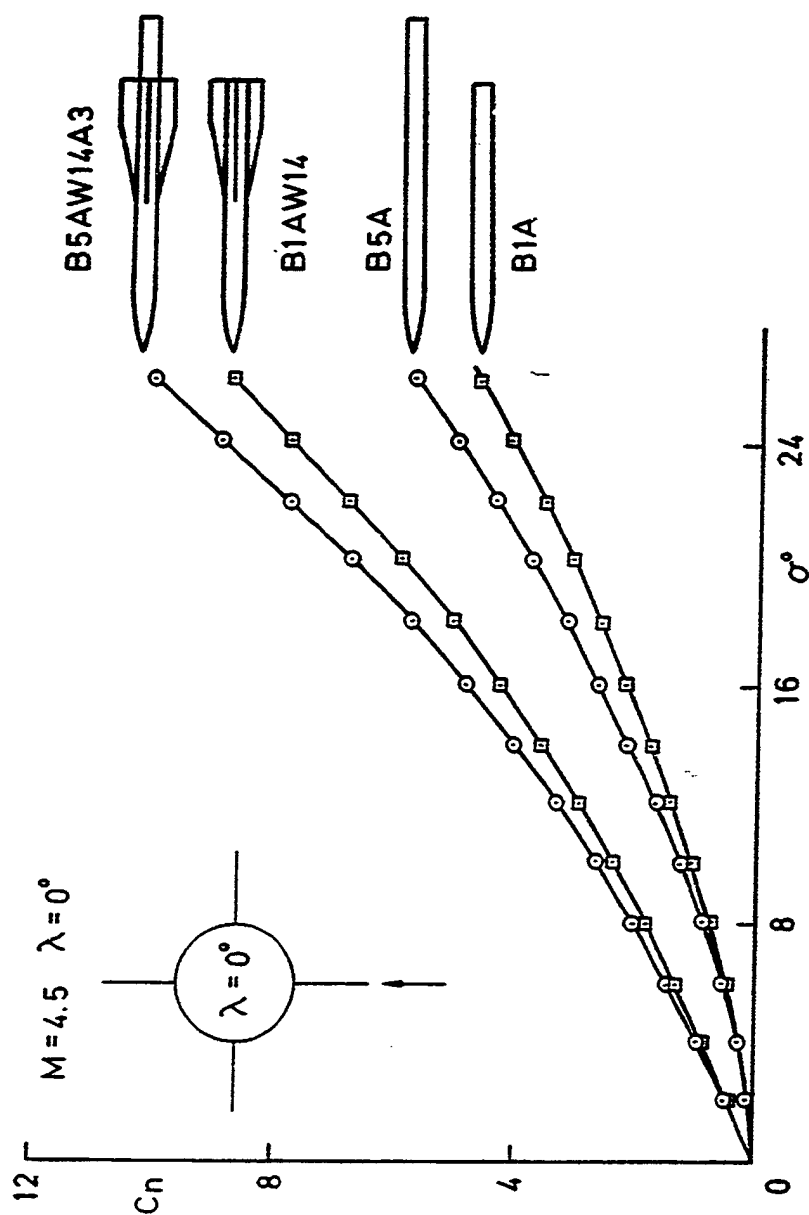


Fig 6 Effect of forebody length on overall normal force, Wing W14

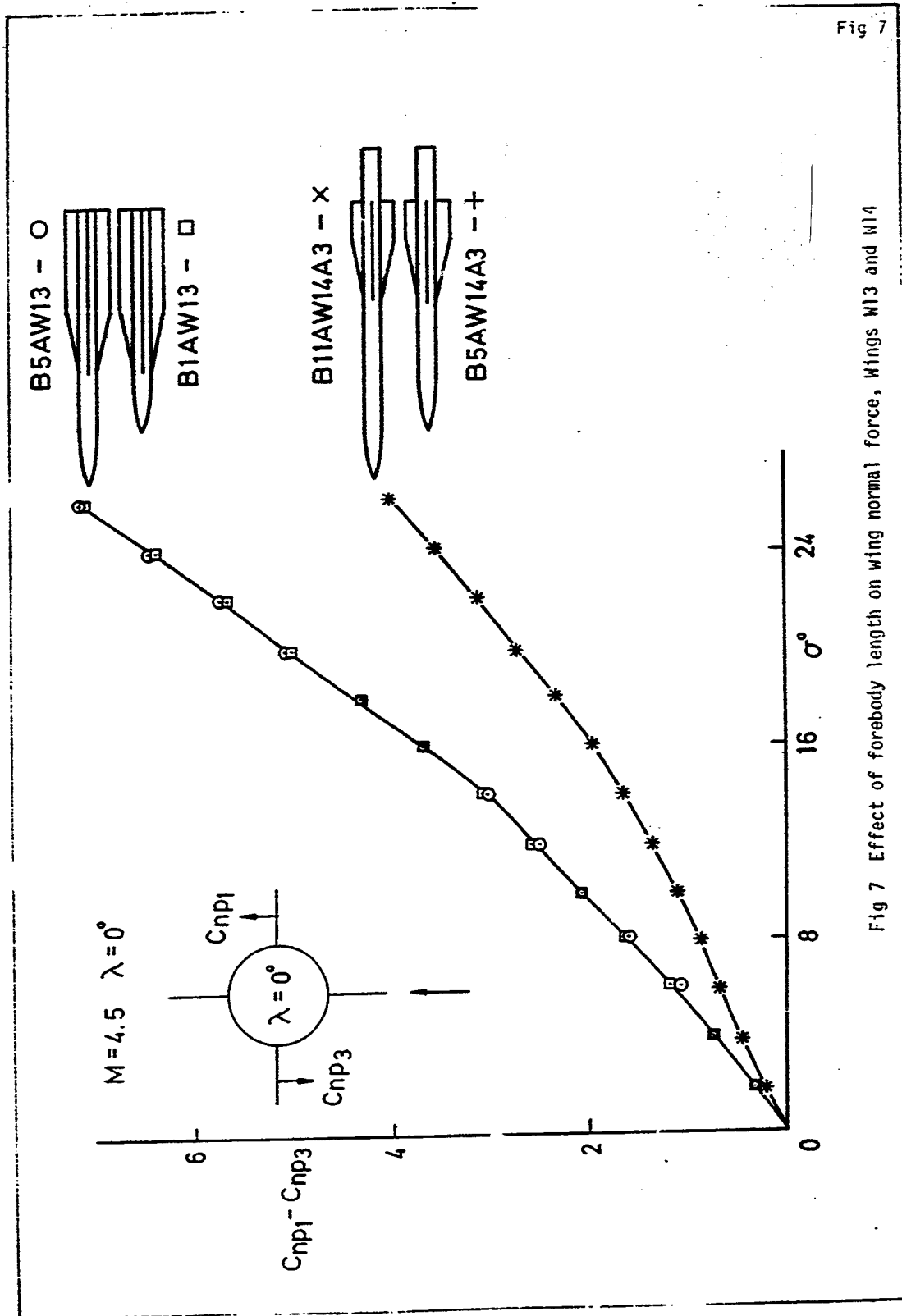


Fig 7

Fig 7 Effect of forebody length on wing normal force, Wings W13 and W14

Fig 8

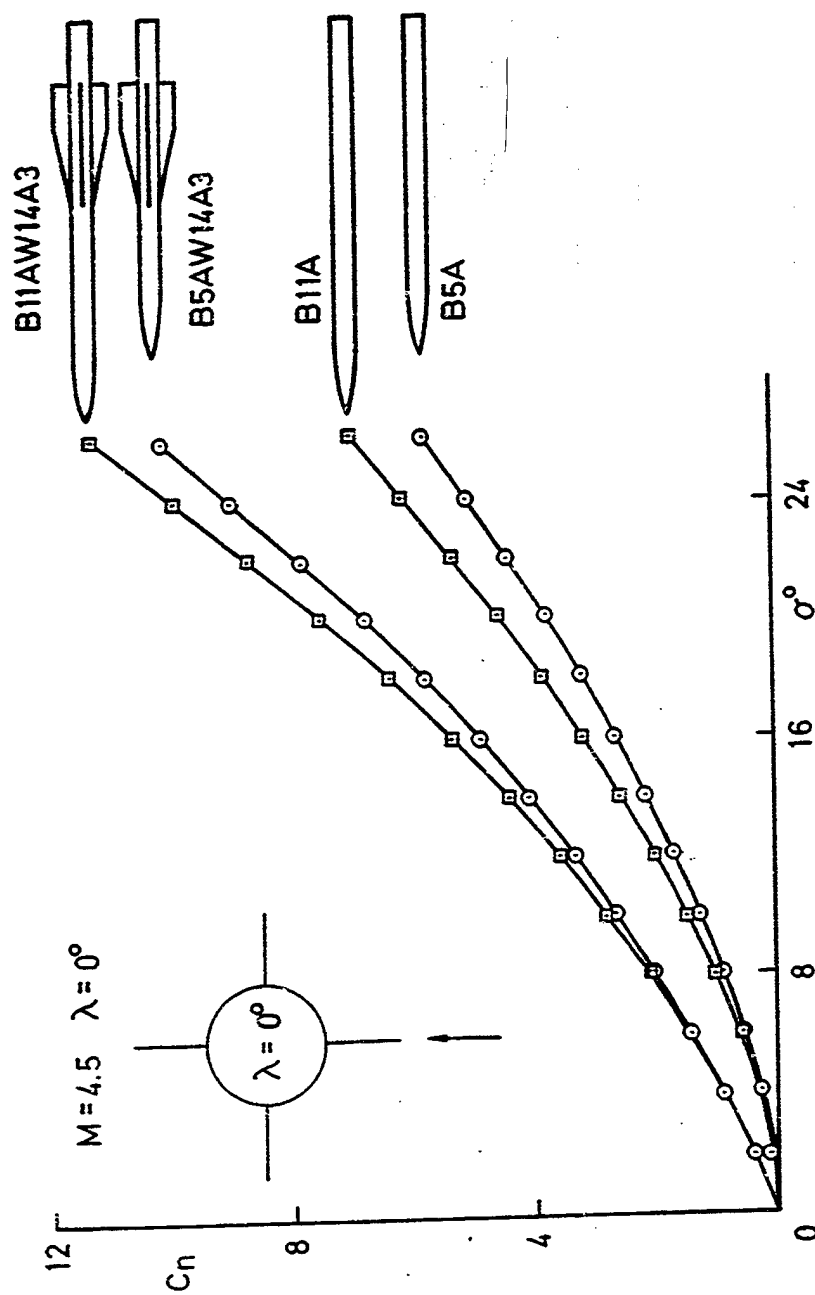


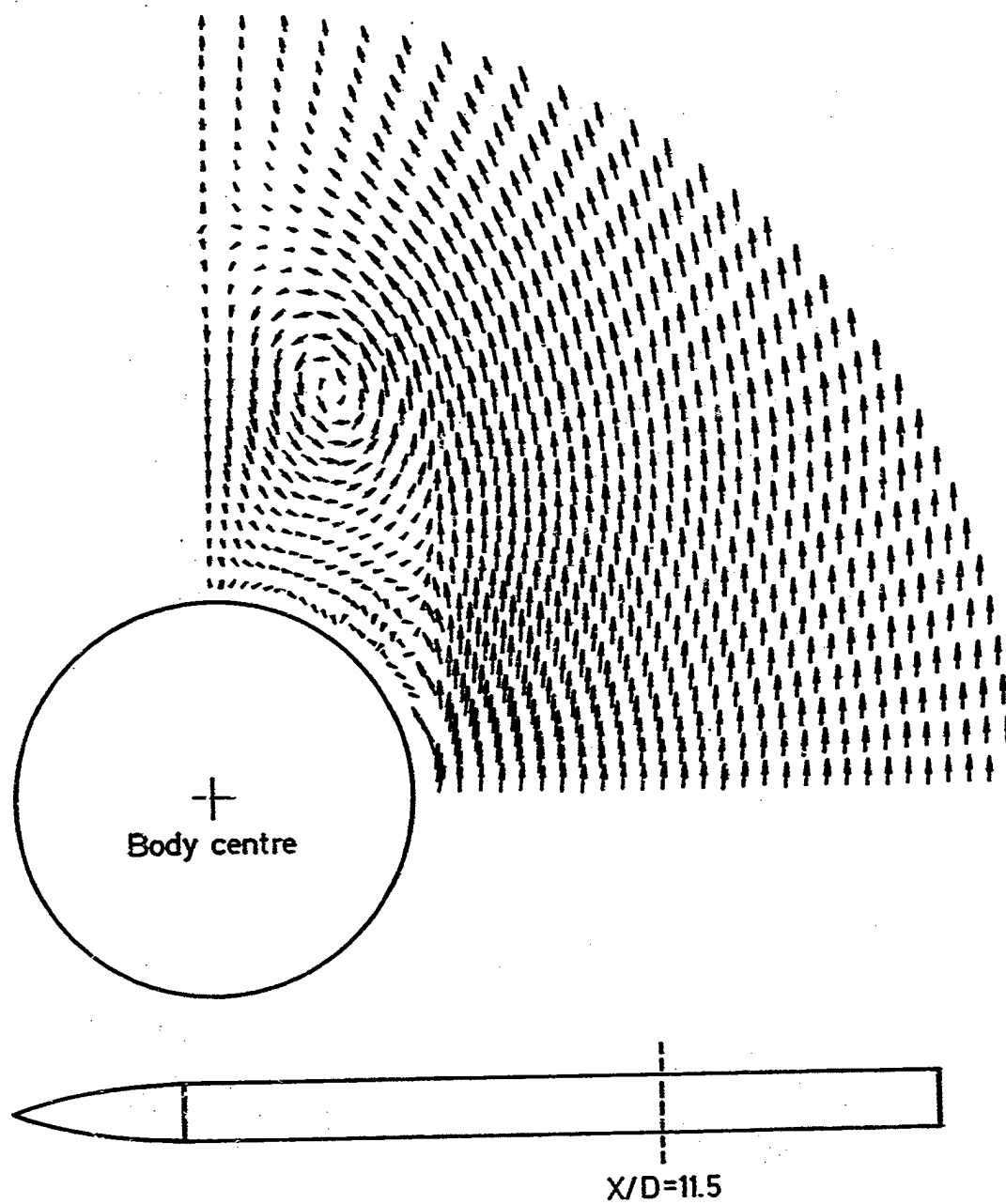
Fig 8 Effect of afterbody length on overall normal force, Wing W14

Fig 9



Fig 9 Flowfield survey rake

Fig 10

Fig 10 Vortex flowfield at $M = 1.8$, $\alpha = 14^\circ$

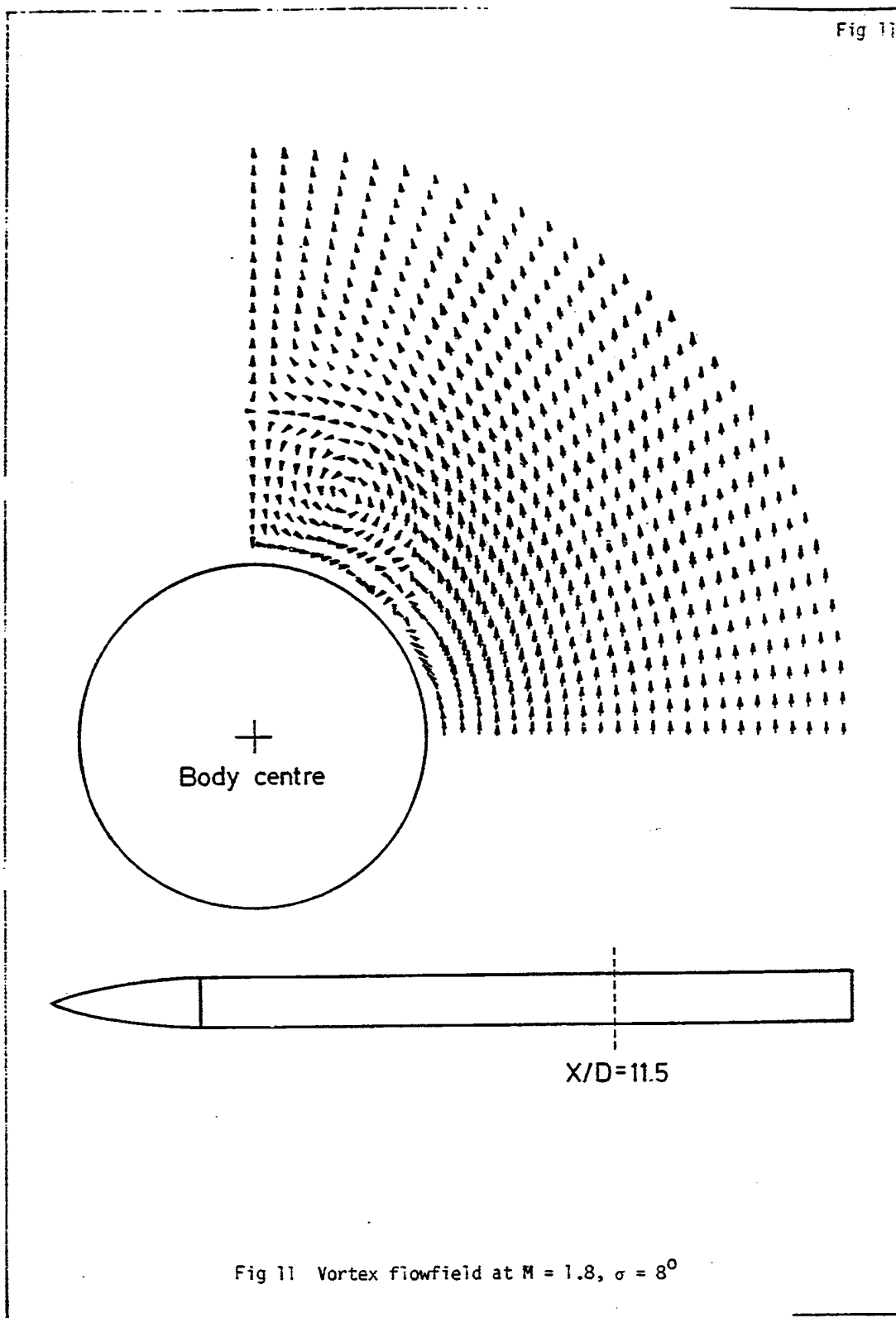


Fig. 12

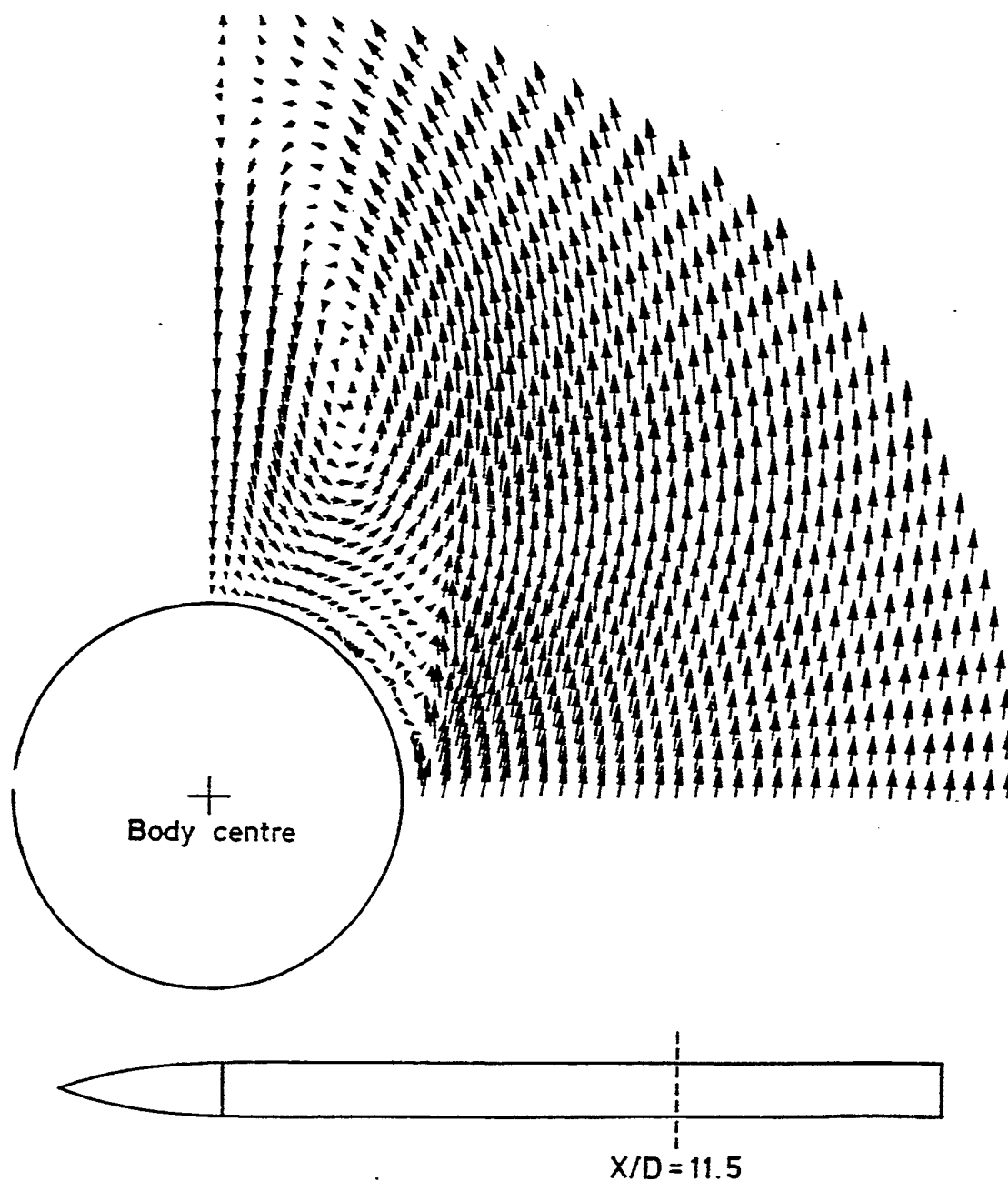


Fig 12 Vortex flowfield at $M = 1.8$, $\alpha = 20^\circ$

Fig 13

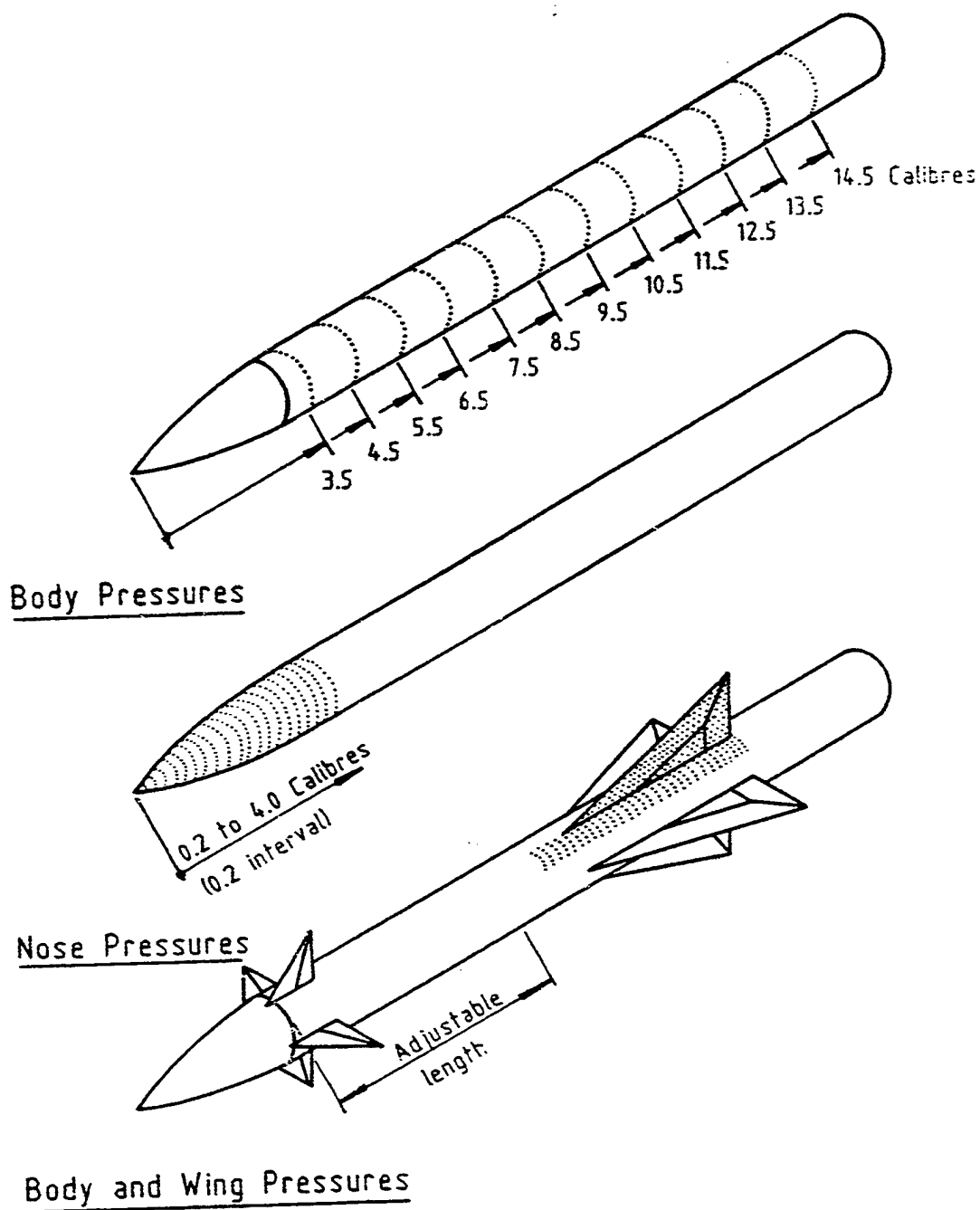


Fig 13 Pressure measurement programme

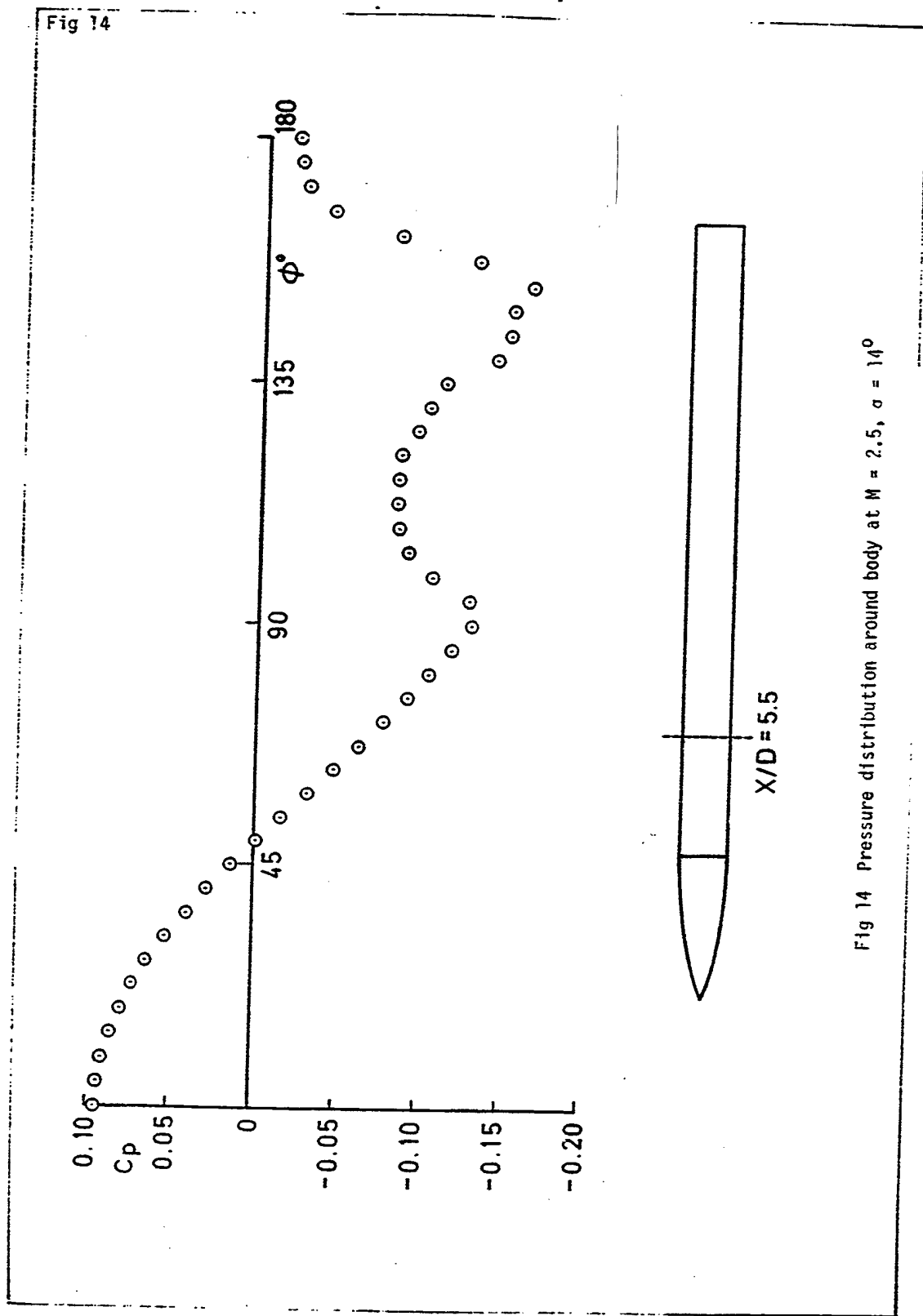


Fig 14 Pressure distribution around body at $M = 2.5$, $\alpha = 14^\circ$

NO 2120

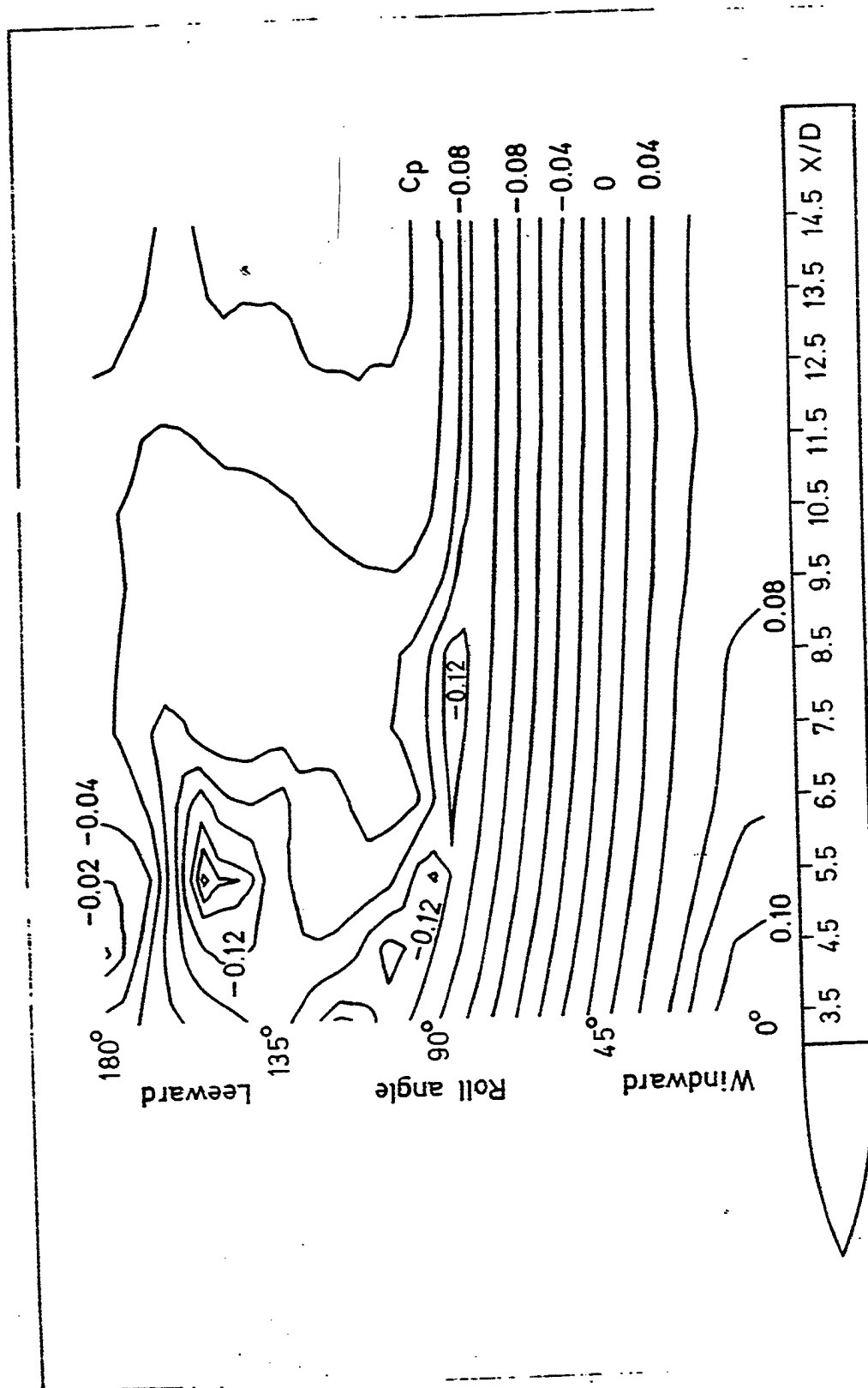


Fig 15

Fig 15 Contours of pressure distribution at $M = 2.5$, $\sigma = 14^\circ$

Fig 16

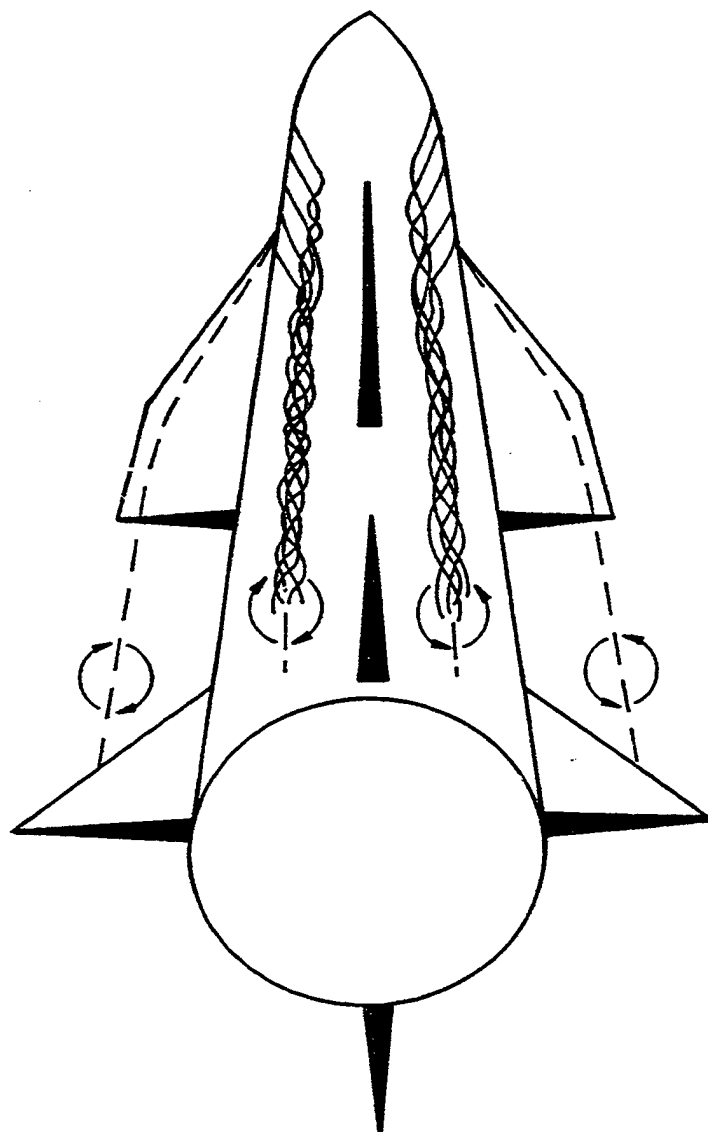


Fig 16 Diagrammatic flow around a missile at a high angle of incidence

Fig 17

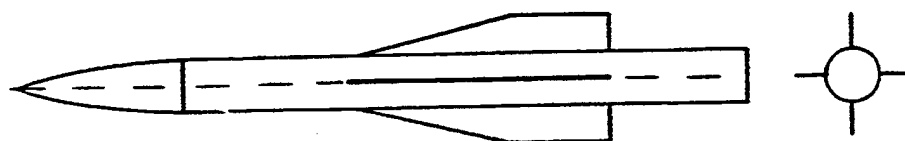
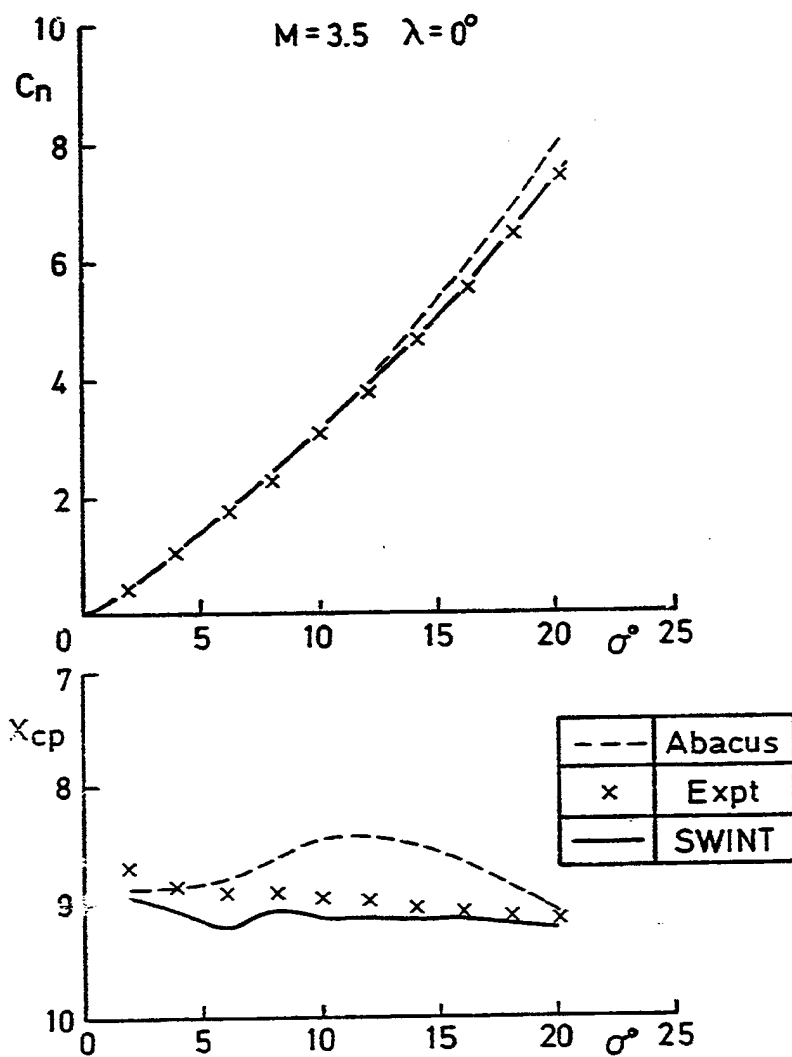


Fig 17 Overall normal force and centre of pressure:
Abacus and SWINT prediction and experiment

Fig 18

$M=3.5 \quad \sigma=12^\circ \quad \zeta=10^\circ$

x	Expt
—	SWINT
- - -	Abacus

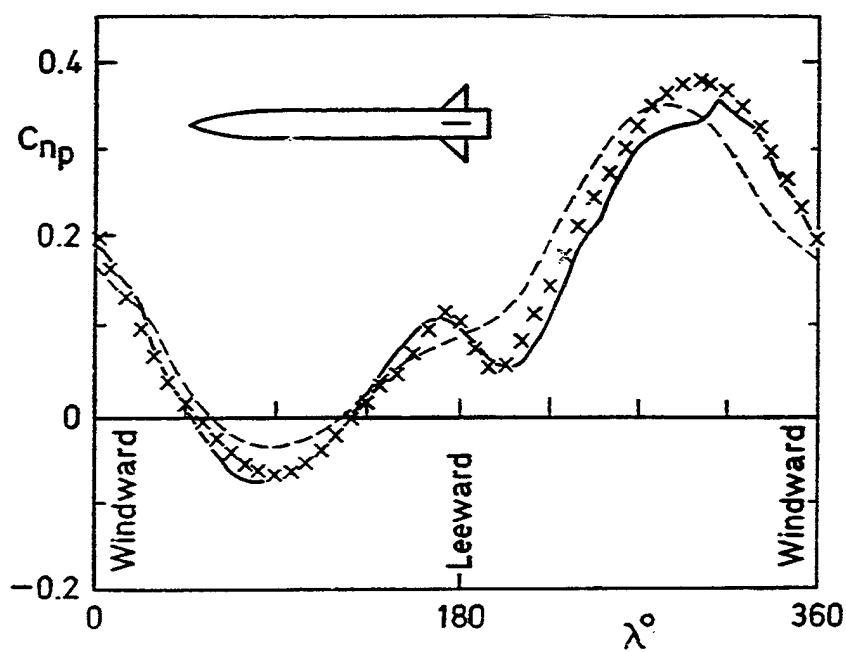


Fig 18 Panel normal force: Abacus and SWINT prediction and experiment

Fig 19

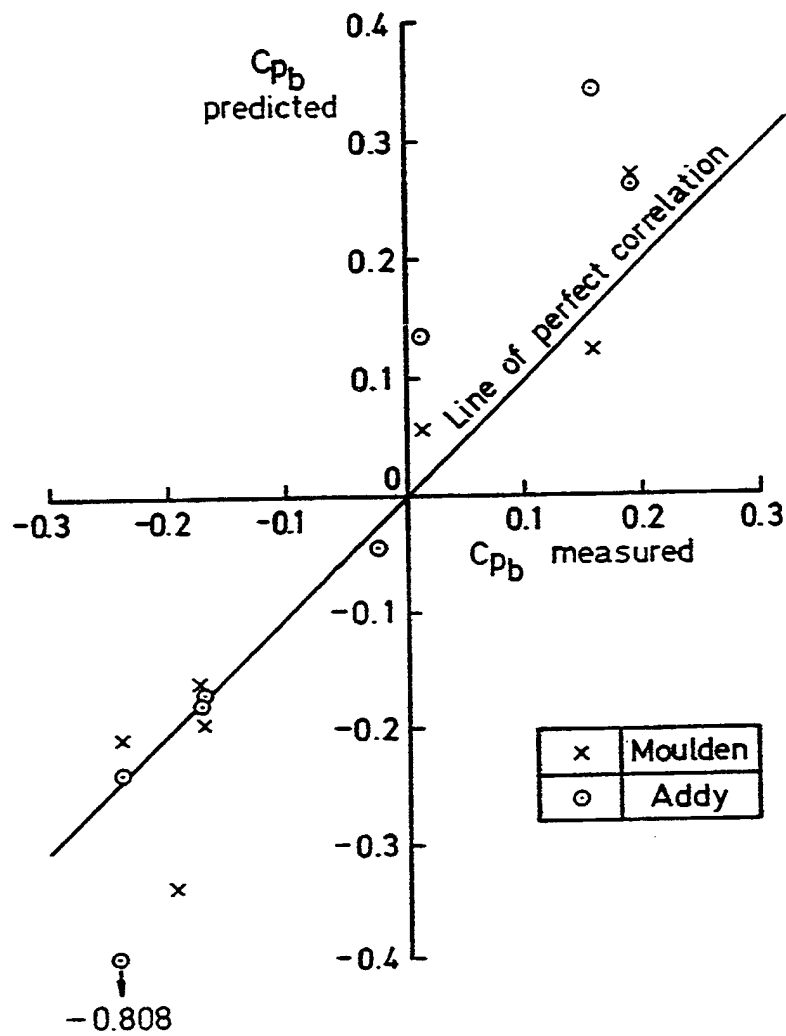


Fig 19 Correlation of predicted and measured base pressures

Fig 20

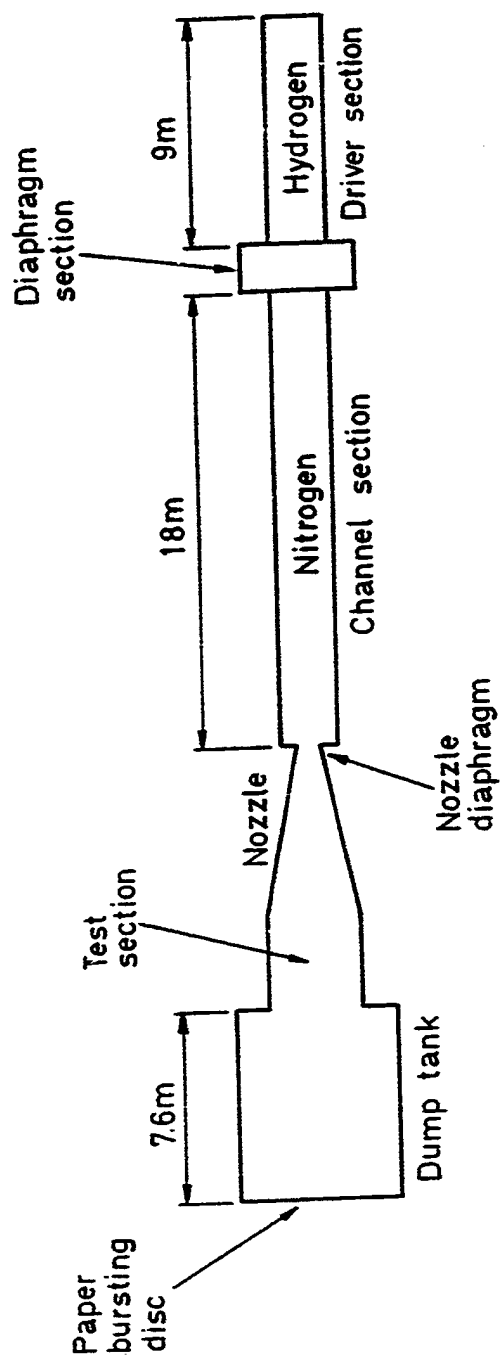


Fig 20 Diagrammatic layout of Shock Tube

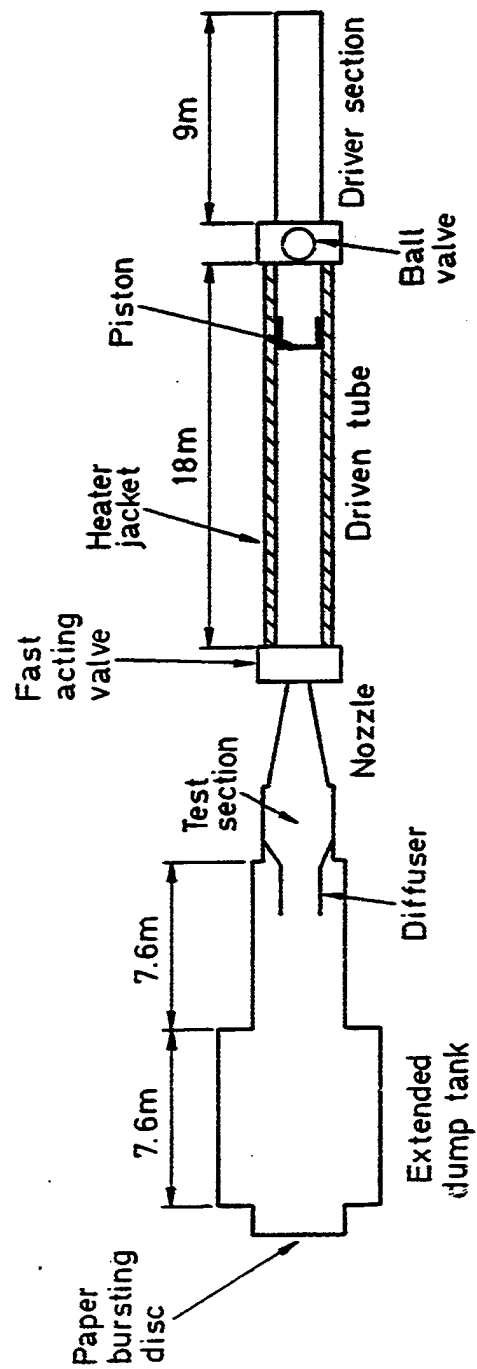


Fig 21

Diagrammatic layout of Shock Tube in LICH mode

Fig 22

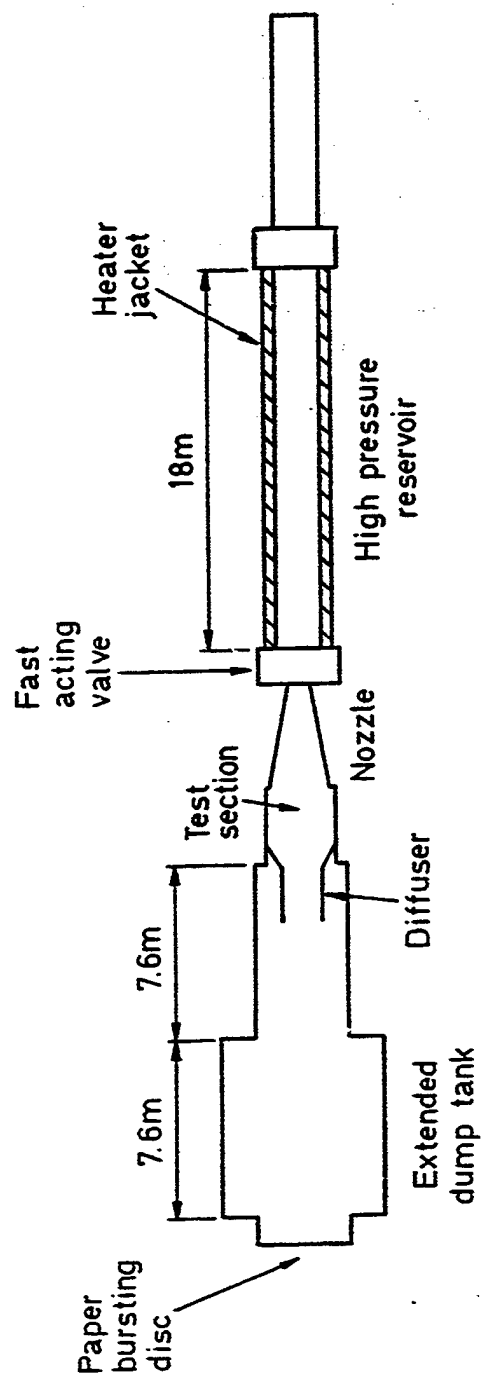


Fig 22 Diagrammatic layout of Shock Tube in Ludwig mode

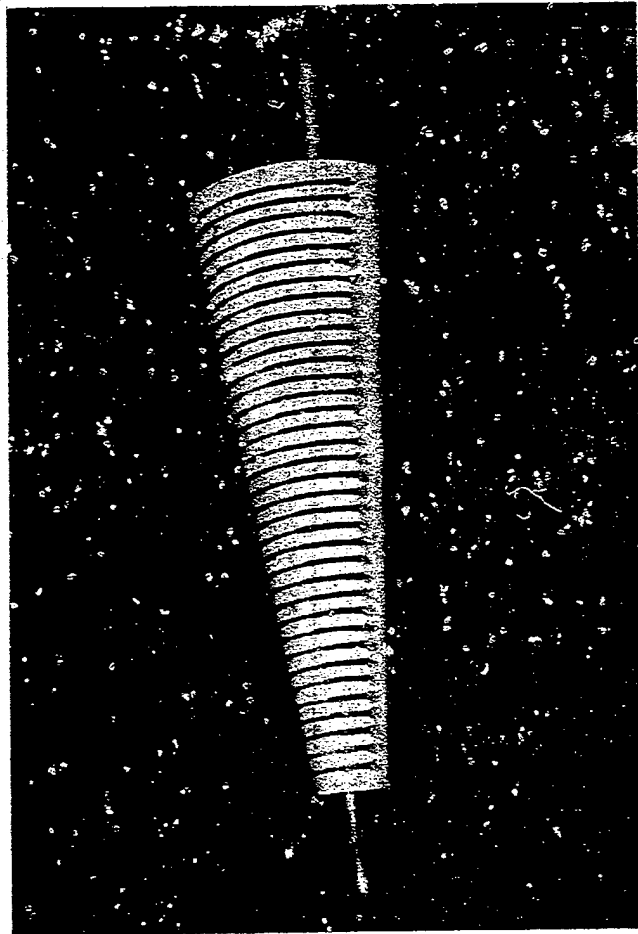


Fig 23 Heat transfer model

Fig 24

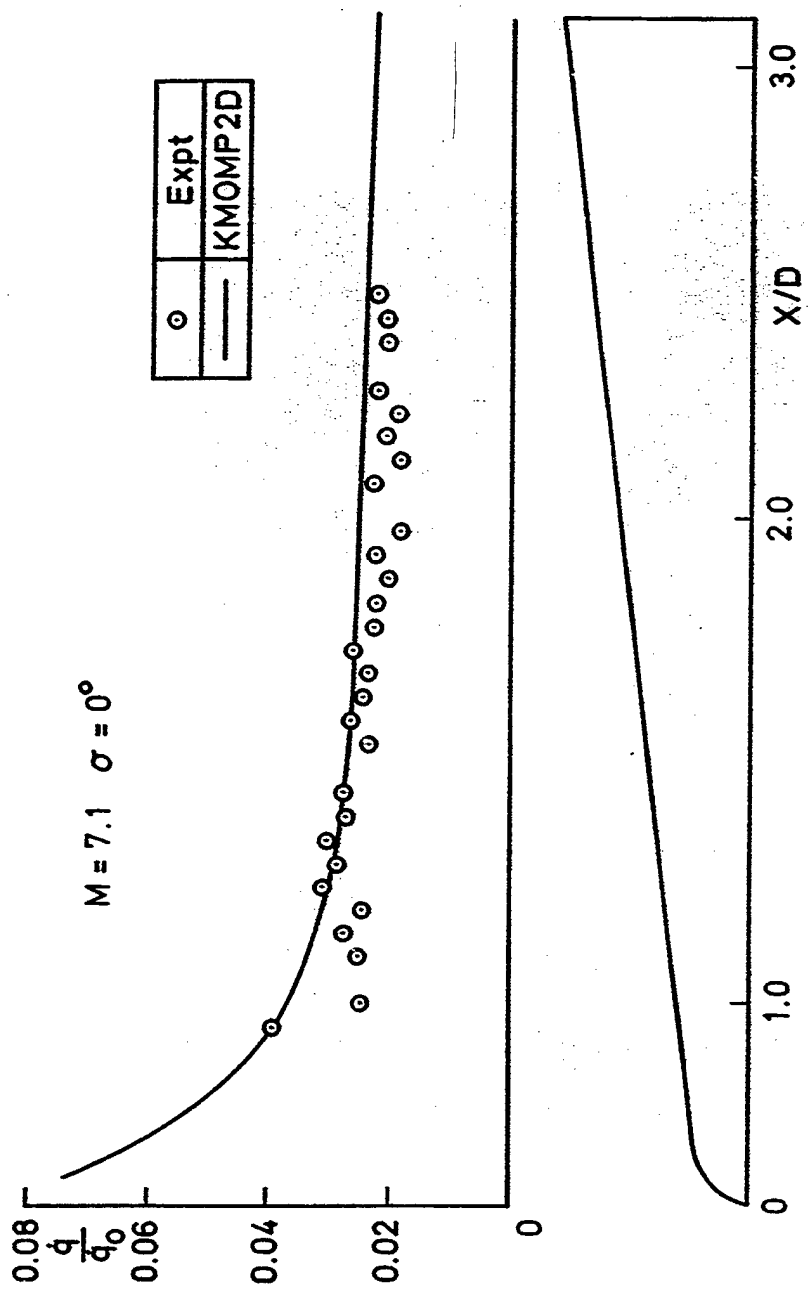


Fig 24 Comparison of measured and predicted heat transfer rates

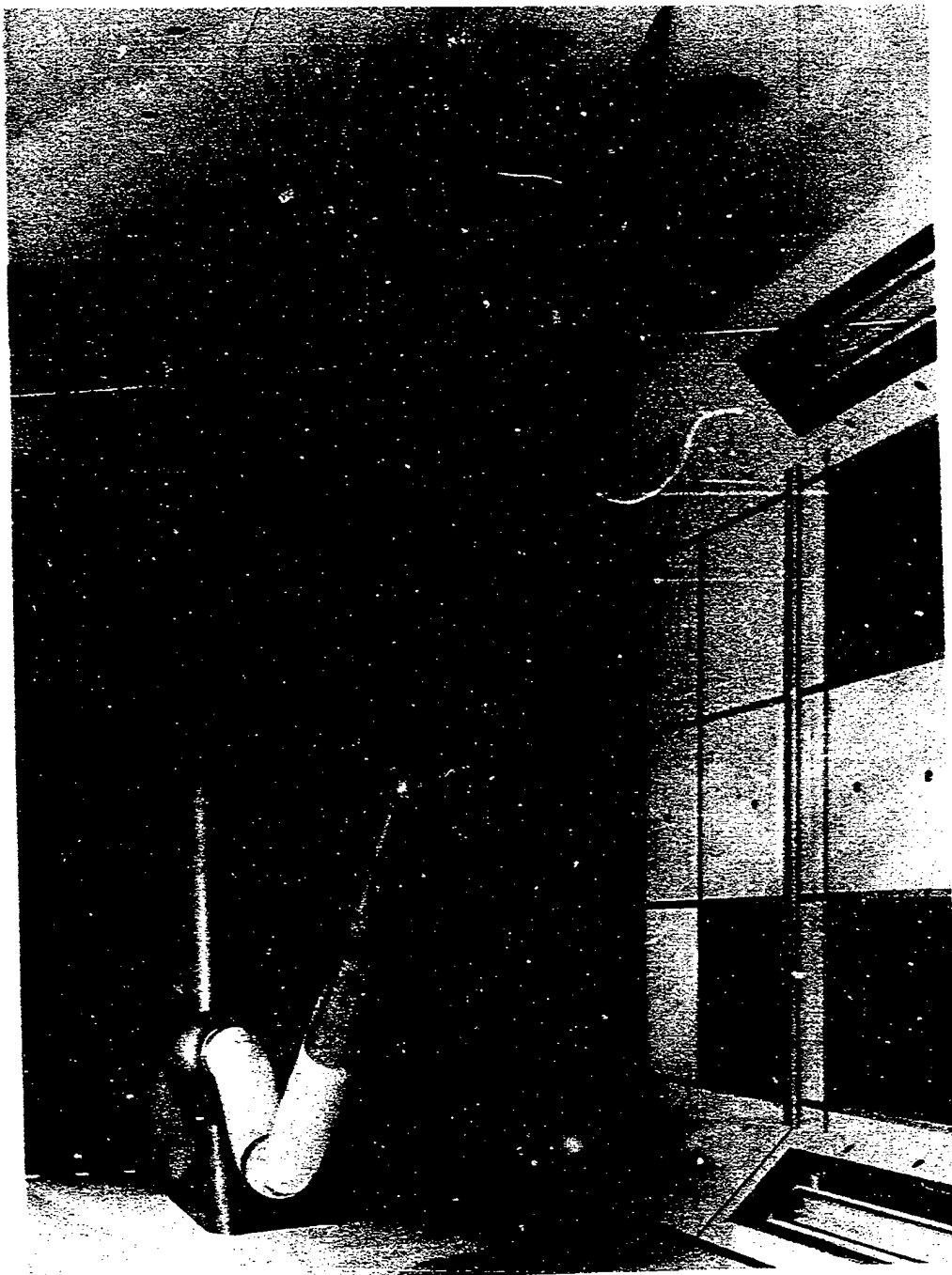


Fig 25 High incidence wind tunnel model

Fig 26

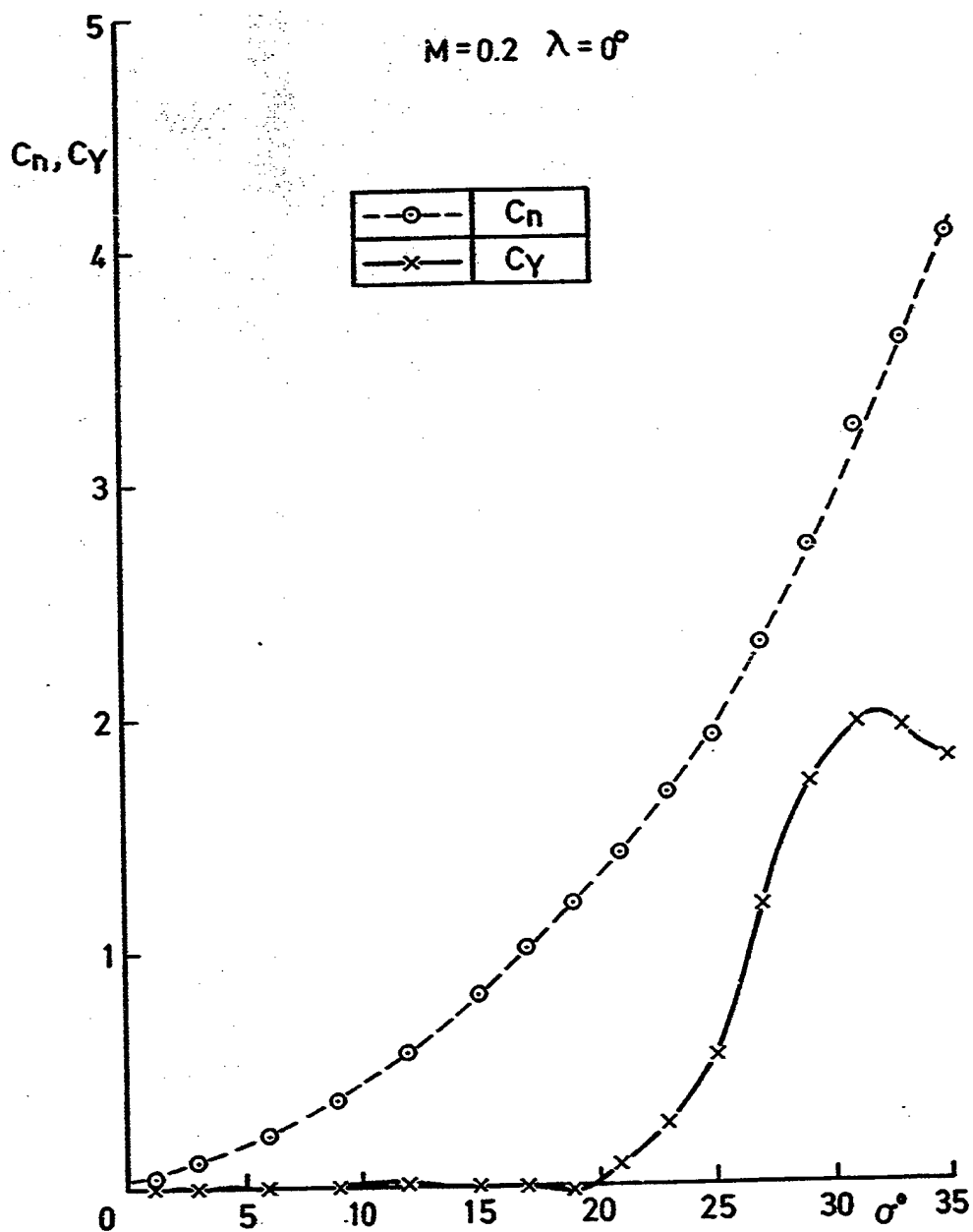


Fig 26 Variation of normal force and side force with angle of incidence

ADS 5042, 3/88, 8068P85.

Ae 2150

Ac 2150

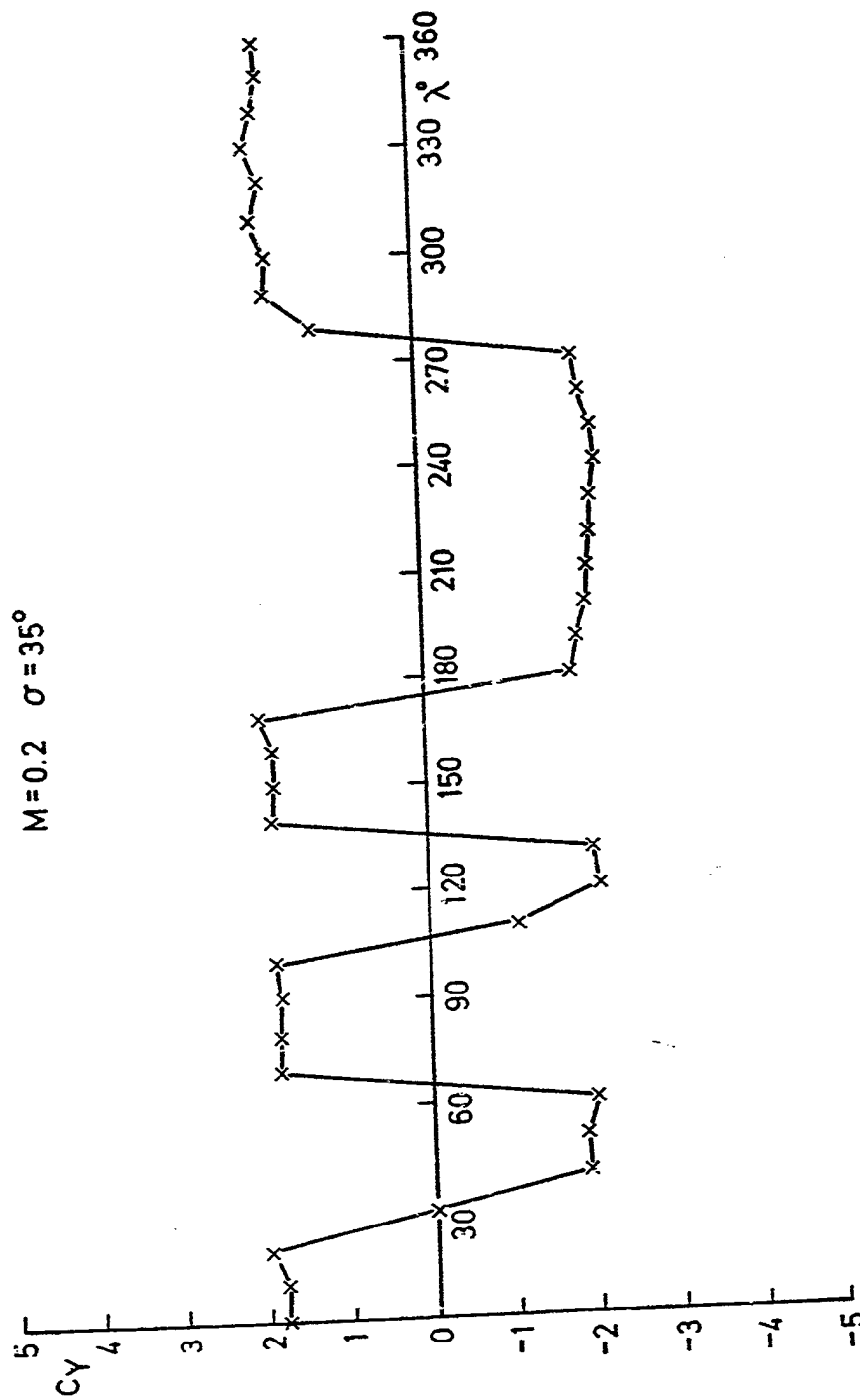


Fig 27

Fig 27 Variation of side force with roll angle

Fig 28

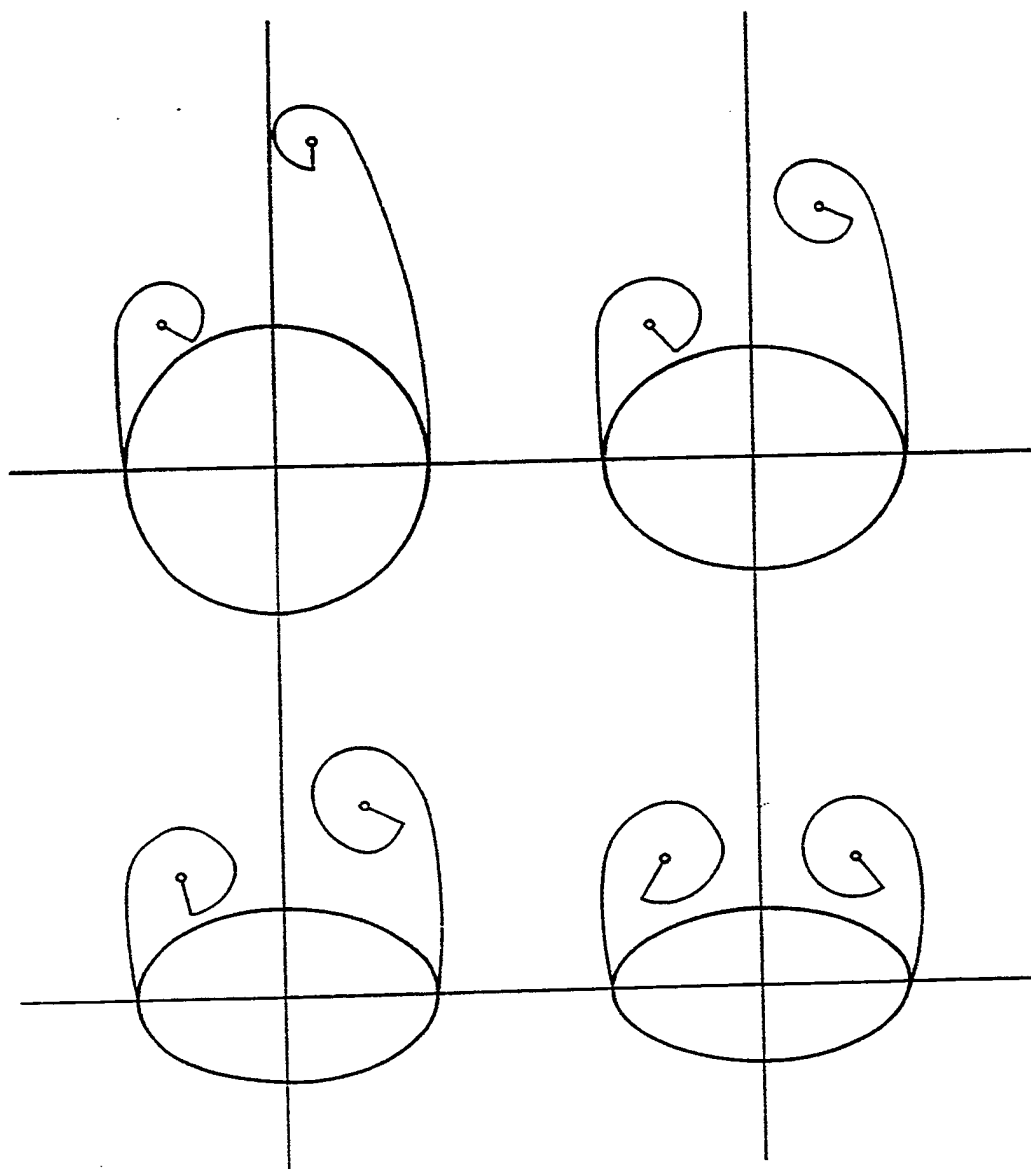
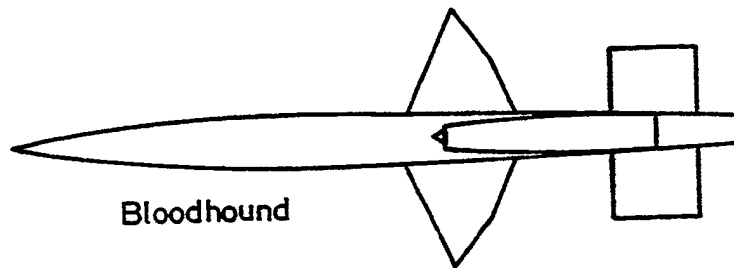
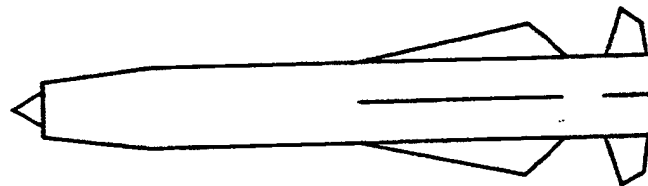


Fig 28 Theoretical vortex configurations for elliptic cones

Fig 29



Bloodhound



Sea Dart

Fig 29 UK air-breathing missiles

Fig 30

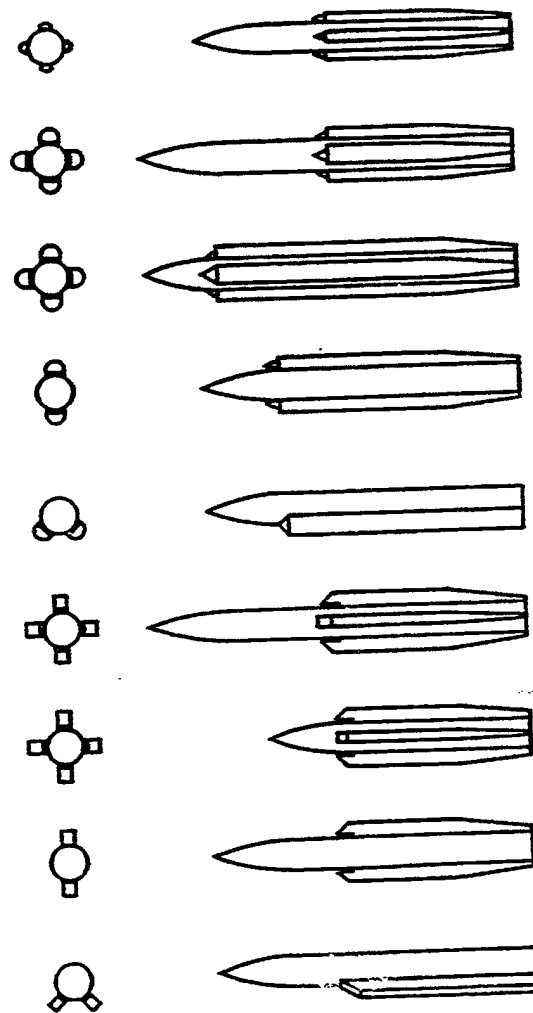


Fig 30 RAE body-intake configurations

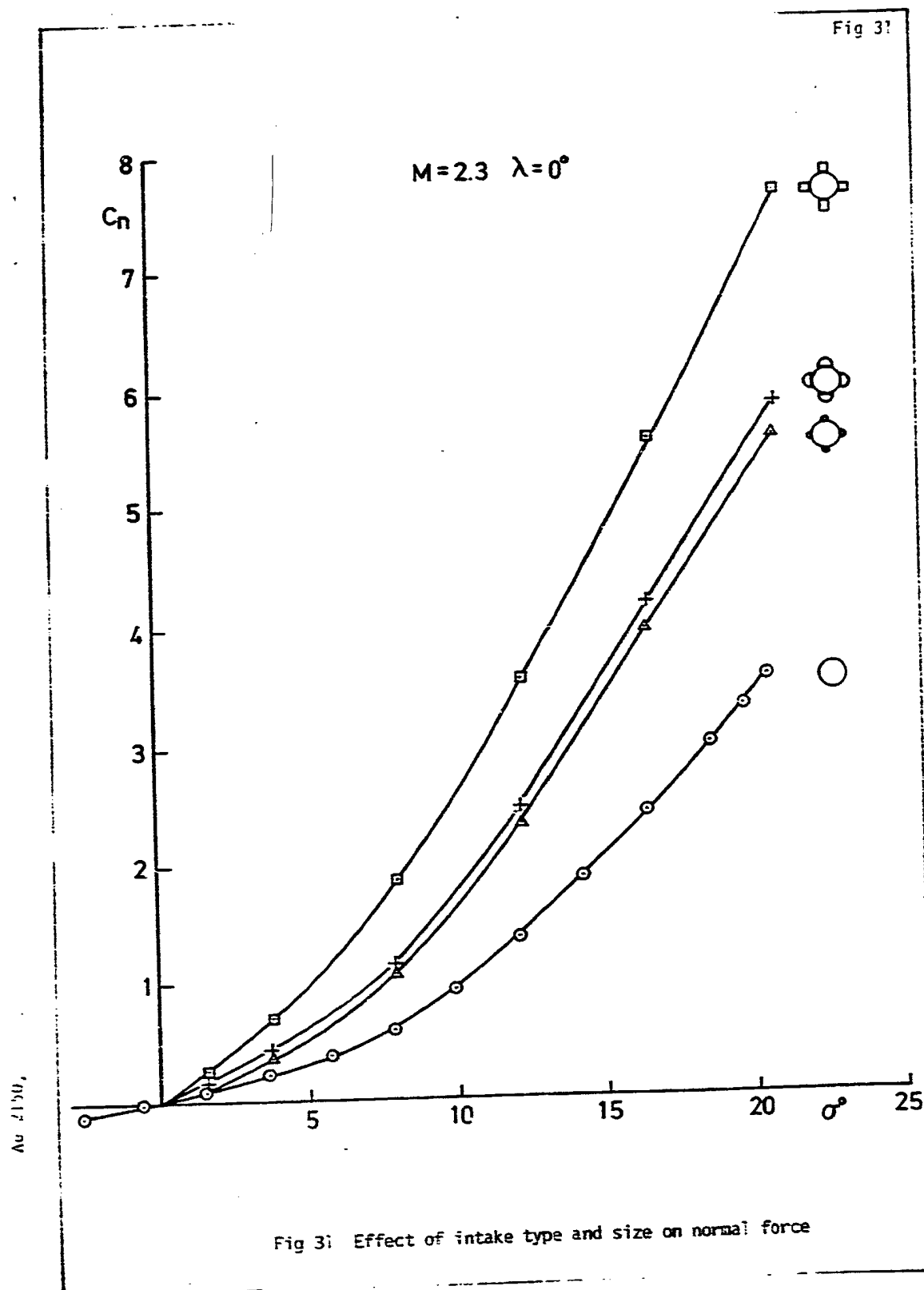


Fig 32

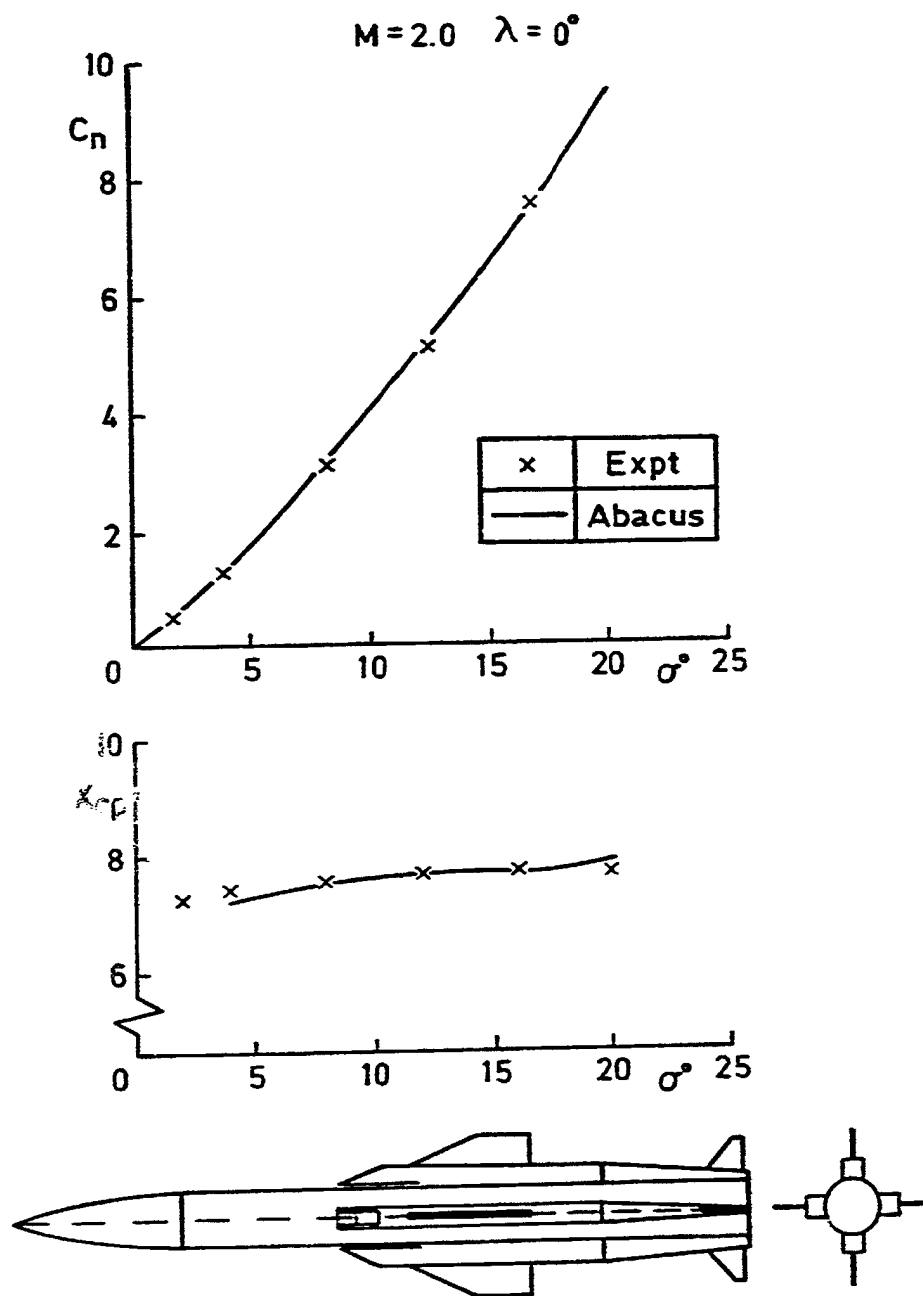
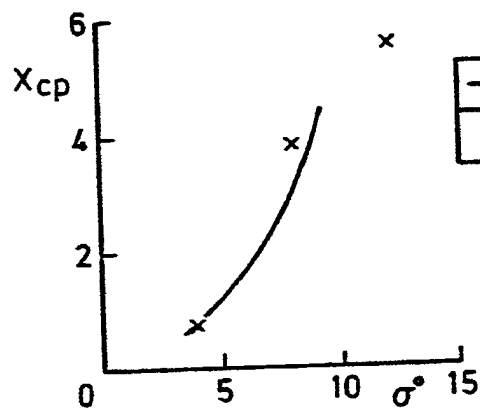
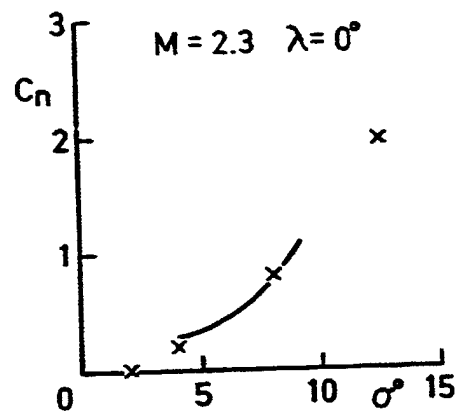


Fig 32 Comparison of Abacus predictions and experiment for 4-intake missile configuration

Fig 33



—	SWINT
x	Expt



Fig 33 Comparison of SWINT predictions and experiment for 2-side-intake missile configuration

Fig 34

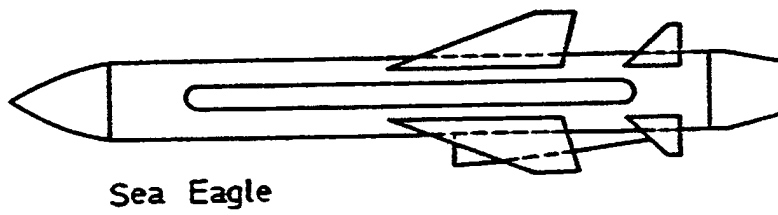


Fig 34 UK air-breathing Stand-Off missile

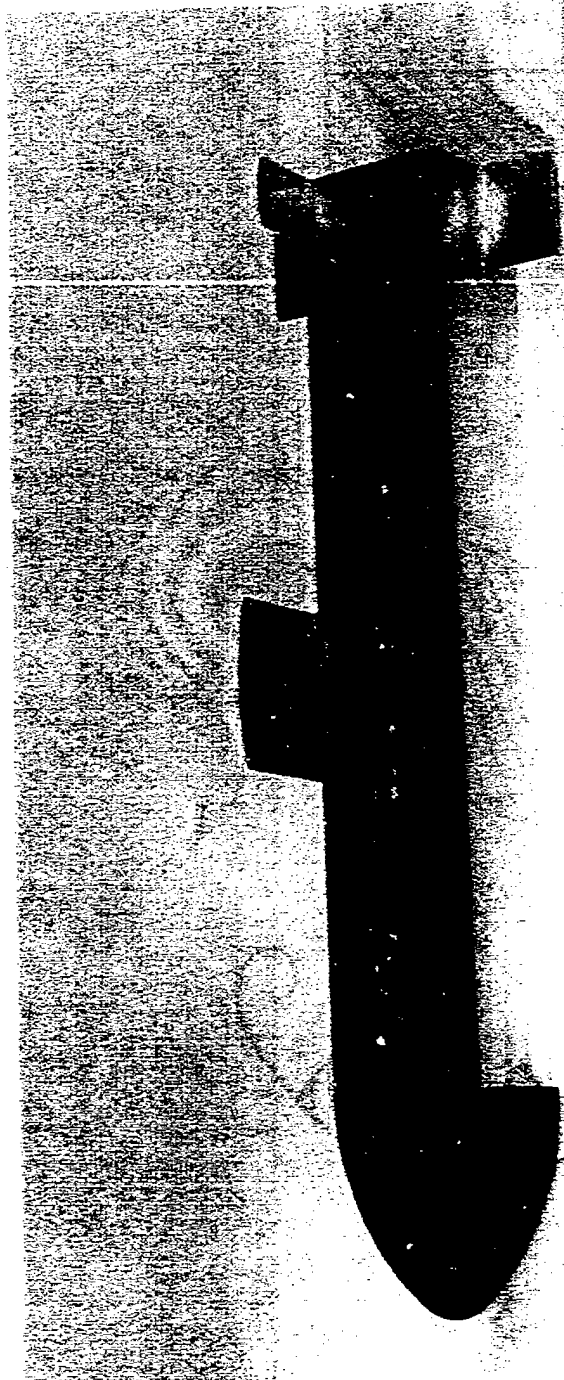
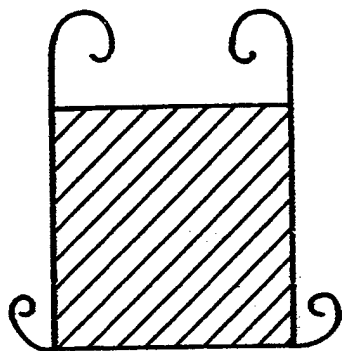


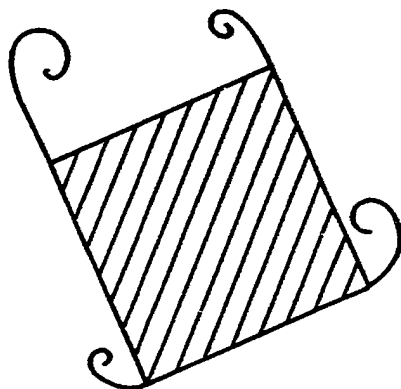
Fig 35

Fig 35 Typical square-bodied weapon

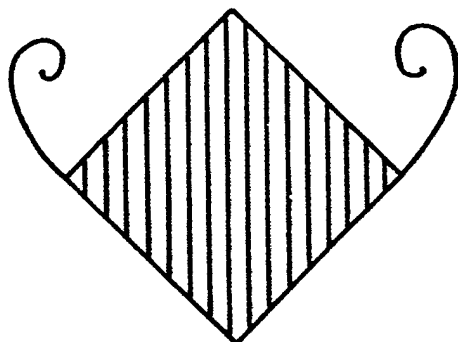
Fig 36



$$\lambda = 0^\circ$$



$$\lambda = 22\frac{1}{2}^\circ$$



$$\lambda = 45^\circ$$

Fig 36 Effect of roll angle on flow around a square body

Fig 37

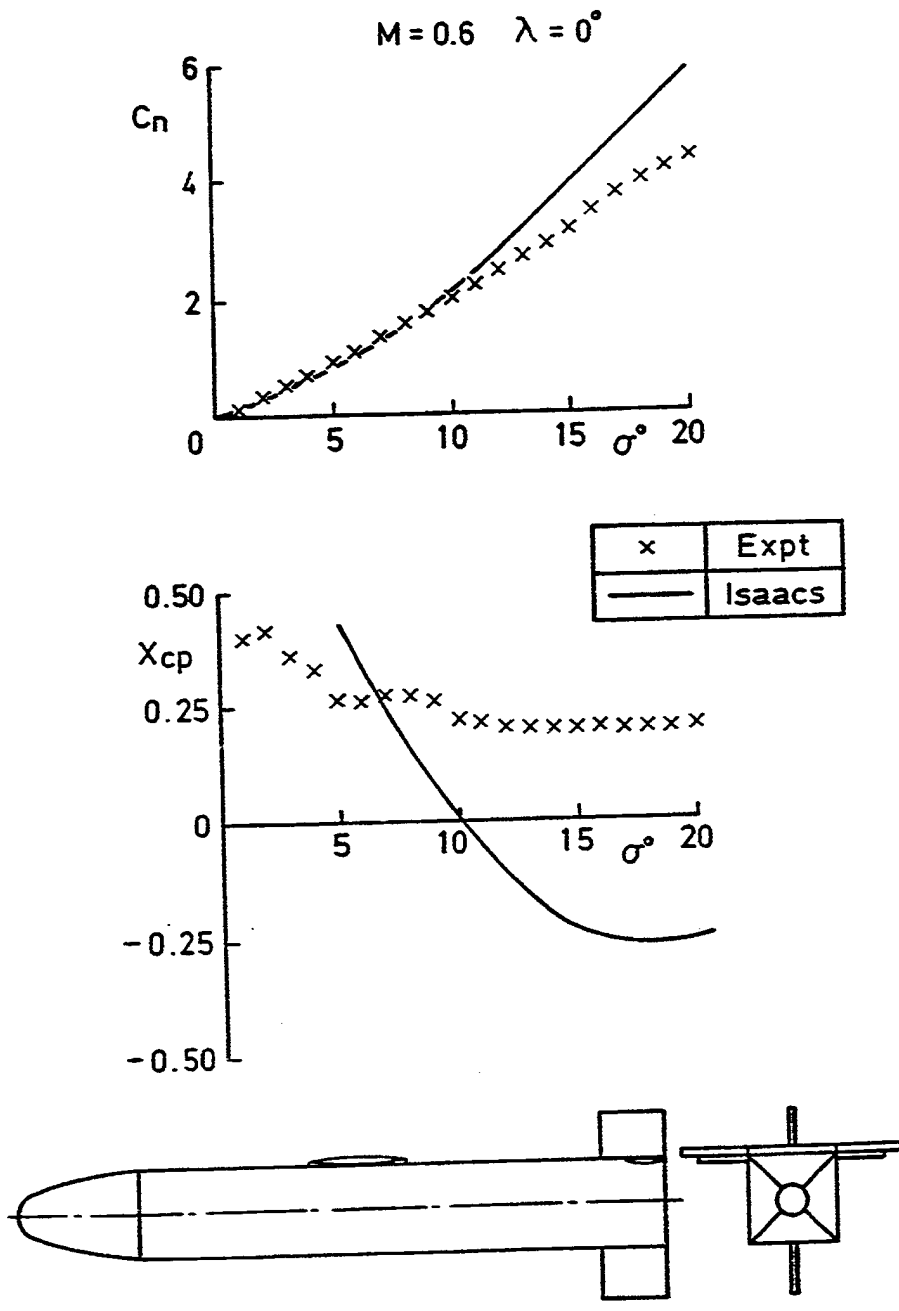


Fig 37 Comparison of predictions and experiment for a square body configuration

Λ 2150

REPORT DOCUMENTATION PAGE

Overall security classification of this page

UNLIMITED

As far as possible this page should contain only unclassified information. If it is necessary to enter classified information, the box above must be marked to indicate the classification, e.g. Restricted, Confidential or Secret.

1. DRIC Reference (to be added by DRIC)	2. Originator's Reference RAE TM Aero 2150	3. Agency Reference	4. Report Security Classification/Marking UNLIMITED		
5. DRIC Code for Originator 7673000W		6. Originator (Corporate Author) Name and Location Royal Aerospace Establishment, Farnborough, Hants, UK			
5a. Sponsoring Agency's Code		6a. Sponsoring Agency (Contract Authority) Name and Location			
7. Title Weapon aerodynamics overview					
7a. (For Translations) Title in Foreign Language					
7b. (For Conference Papers) Title, Place and Date of Conference					
8. Author 1. Surname, Initials Foster, D.N.	9a. Author 2	9b. Authors 3, 4	10. Date January 1989	Pages 59	Refs. 25
11. Contract Number	12. Period	13. Project	14. Other Reference Nos.		
15. Distribution statement (a) Controlled by - (b) Special limitations (if any) - If it is intended that a copy of this document shall be released overseas refer to RAE Leaflet No.3 to Supplement 6 of MOD Manual 4.					
16. Descriptors (Keywords) (Descriptors marked * are selected from TEST)					
17. Abstract The objective of this Memorandum is to highlight the problems currently facing the weapon aerodynamicist; the origins of these problems, and the methods available to predict and to solve the problems.					